

NANOBIOTECHNOLOGICAL APPLICATIONS OF S-LAYERS

EVA MARIA EGELSEER*,
NICOLA ILK, DIETMAR PUM,
PAUL MESSNER, CHRISTINA
SCHÄFFER, BERNHARD
SCHUSTER, and UWE B.
SLEYTR,
Center for NanoBiotechnology,
University of Natural
Resources and Applied Life
Sciences Vienna, Austria

Keywords: crystalline surface layers; S-layers; S-layer fusion proteins; S-layer neoglycoproteins; self-assembly; bottom-up strategy; nanobiotechnology; molecular construction kit

INTRODUCTION

Crystalline bacterial cell surface layers, termed *S-layers* (1, 2), are one of the most commonly observed outermost cell envelope structures of prokaryotic organisms (Bacteria and Archaea). These monomolecular isoporous structures, composed of a single protein or glycoprotein species, represent the simplest protein membranes developed during evolution. Most importantly, isolated S-layer (glyco)proteins possess the intrinsic property for recrystallization into isoporous lattices in suspension and at a broad range of surfaces (e.g. polymers, silicon, and metals) and interfaces (e.g. air–liquid interface, lipid films, and liposomes).

Since one of the key challenges in biotechnology and material sciences is the technological utilization of self-assembly systems, wherein molecules spontaneously associate into defined supramolecular structures, S-layers have a great potential as patterning elements. The well-defined arrangement of functional groups on S-layer lattices and the repetitive physicochemical properties down to the nanometer scale allow the binding of functional molecules (e.g. enzymes, antibodies, antigens, and ligands) and nanoparticles with unsurpassed spatial control. Moreover, S-layers can be used as structural basis for a biomolecular construction kit involving all major species of biological molecules (proteins, lipids, glycans, nucleic acids, and combinations of these).

The possibility of modifying and changing the natural properties of S-layer proteins by genetic engineering techniques and to incorporate specific functional domains while maintaining the self-assembling capability have led to new types of ultrafiltration membranes, affinity structures, enzyme membranes, microcarriers, biosensors, diagnostic devices, biocompatible surfaces, vaccines, as well as targeting, delivery, and encapsulation systems.

*Corresponding author: Center for NanoBiotechnology, University of Natural Resources and Applied Life Sciences Vienna, Austria. Email: Egeleseer@groupwise.boku.ac.at

In this article, a survey of the general principles of S-layers and their application in molecular nanotechnology, nanobiotechnology, and biomimetics is given (3–10).

GENERAL ASPECTS OF S-LAYERS

Occurrence, Location, Structure, and Assembly

In the course of evolution, prokaryotic organisms developed a great diversity in the supramolecular architecture of their multilayered cell boundary (Fig. 1) (11). One of the most common features of prokaryotic cell envelopes is the presence of a monomolecular array of protein or glycoprotein subunits referred to as *surface (S-) layer* (2, 12). The identification of S-layers on selected organisms led to the assumption that these structures represent a rather unique cell envelope component (1, 13), but until now, they have been identified in hundreds of different species belonging to all major phylogenetic groups of bacteria and represent an almost universal feature of archaea (14–17).

Despite the observation that remarkable variation exists in the structure and chemical composition of prokaryotic cell envelopes, S-layers as essential component must have coevolved with these structures. In most archaea, the S-layer is integrated into the plasma membrane (Fig. 1a). In gram-positive bacteria and in archaea, the S-layer lattice assembles on the surface of the rigid wall matrix, which is mainly composed of peptidoglycan and secondary cell wall polymers (SCWPs) or pseudomurein, respectively (Fig. 1b). In gram-negative bacteria, the S-layer is attached to the lipopolysaccharide (Fig. 1c). Some bacteria can assemble two superimposed S-layers, each composed of a different subunit species (14).

High resolution electron microscopical studies revealed that S-layer lattices can have oblique (p1, p2), square (p4), or hexagonal (p3, p6) symmetry (Fig. 2), with a center-to-center spacing of the morphological units of approximately 3–35 nm. Amongst archaea, hexagonal symmetry is predominant (11, 14, 16).

Depending on the lattice type, the morphological units constituting S-layers consist of one, two, three, four, or six identical (glyco)protein subunits. High resolution structural studies by electron and scanning probe microscopy in combination with permeability studies revealed that S-layers are porous protein meshworks with pores occupying ~70% of the surface area. The pores within S-layer lattices are of identical size (usually in the 2–8 nm range) and shape. Often, two or more distinct classes of pores are present (Fig. 2). As monomolecular arrays, S-layers are generally 5–25 nm thick and reveal a rather smooth outer and a more corrugated inner surface (18–20). In S-layer lattices of archaea, pillar-like domains on the inner surface can often be identified, which protrude into the plasma membrane (Fig. 1a). In many species of bacteria, the S-layers of individual strains exhibit great diversity with respect to lattice symmetry and lattice constants. As confirmed by genetic and chemical studies, S-layers are nonconservative structures and, consequently, only of limited taxonomical value. Even individual strains of selected

2 NANOTECHNOLOGICAL APPLICATIONS OF S-LAYERS

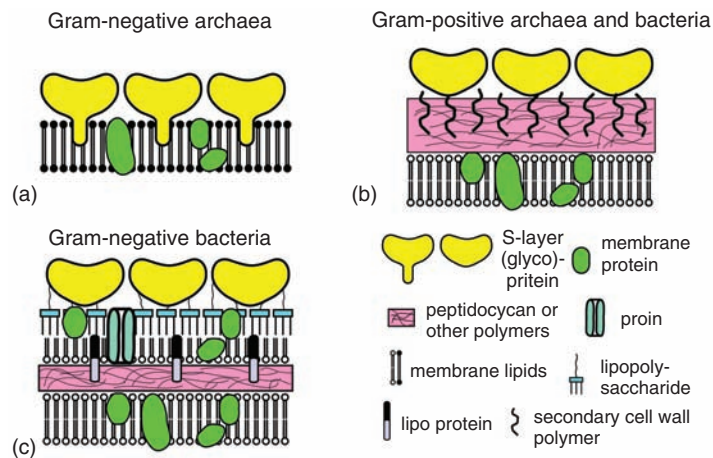


Figure 1. Schematic illustration of the supramolecular architecture of the three major classes of prokaryotic cell envelopes containing crystalline bacterial cell surface layers (S-layers). (a) Cell envelope structure of gram-negative archaea with S-layers as the only cell wall component external to the cytoplasmic membrane. (b) Cell envelope as observed in gram-positive archaea and bacteria. In bacteria, the rigid wall component is primarily composed of peptidoglycan. In archaea, other wall polymers (e.g. pseudomurein or methanochondroitin) are found. (c) Cell envelope profile of gram-negative bacteria composed of a thin peptidoglycan layer and an outer membrane. If present, the S-layer is closely associated with the lipopolysaccharide of the outer membrane.

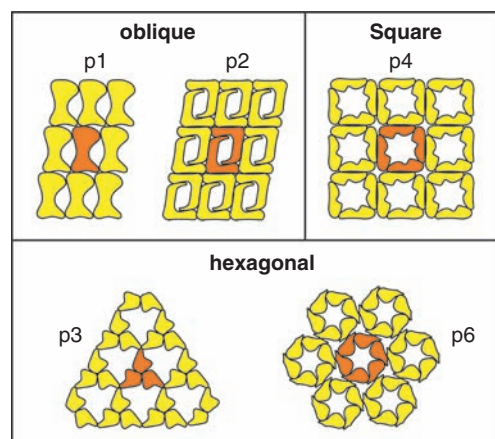


Figure 2. Schematic drawing of the five different S-layer lattice types. The regular arrays exhibit oblique (p1, p2), square (p4), or hexagonal lattice symmetry (p3, p6). The morphological units are composed of one, two, three, four, or six identical subunits.

species often reveal the capability of synthesizing different S-layer (glyco)proteins.

The most accurate picture of the structure and orientation of S-layers on intact cells can be obtained by freeze-fracture replication of shock-frozen and deep-etched cell suspensions (Fig. 3) (1, 11, 21). By the application of this technique, it has been demonstrated that S-layers completely cover bacterial cell surfaces. From the observation it can be calculated that approximately 5×10^5 S-layer protein monomers are needed to cover an average size rod-shaped prokaryotic cell. Consequently, at short generation times of about 20 min, the cell has to synthesize approximately 500 S-layer subunits per second for maintaining an S-layer lattice on its surface (22). After secretion, the subunits of most S-layers interact with each other and with the supporting layer through noncovalent forces.



Figure 3. Electron micrograph of a freeze-etched preparation of an intact cell of *Lysinibacillus sphaericus* CCM 2177 showing a square (p4) S-layer lattice that completely covers the cell surface.

Differences in the net charges of both surfaces and specific interactions between either the N- or C-terminal part of the S-layer protein and the supporting envelope layer have been shown to be responsible for the proper orientation of the S-layer on the cell surface in the course of lattice growth (21, 23).

Since bacteria and archaea carrying S-layers are ubiquitous in the biosphere and dwell in the most diverse habitats, they fulfill a broad spectrum of functions (15–17, 24) such as acting as a (i) structure involved in cell adhesion and surface recognition, (ii) protective coats, molecular sieves, and molecule and ion traps, and (iii) virulence factor in pathogenic organisms. In archaea that possess S-layers as the exclusive wall component, S-layer (glyco)protein lattices determine cell shape and the cell fission process.

S-layers can usually be disrupted into their constituent subunits by chaotropic agents (e.g. urea and guanidinium hydrochloride) or by lowering or raising the pH value. Upon removal of the disrupting agent (e.g. by dialysis), the isolated S-layer subunits reassemble into monomolecular crystalline arrays in solution (21, 25, 26), on solid supports (e.g. polymers, silicon wafers, metals) (7, 27, 28), at the air–water interface (29), on planar lipid films or on liposomes (5, 25, 26, 30), and nanocapsules (31).

Crystal growth at surfaces and interfaces is initiated at randomly distributed nucleation sites composed of small protein assemblies from bulk solution. The crystalline domains subsequently grow laterally in all directions until neighboring areas meet and a closed coherent monolayer is formed (15, 28, 32, 33).

Although the S-layer lattice exhibits a polycrystalline character, the individual crystalline domains have the same orientation with respect to the interface. Patterned S-layer lattices on solid supports can be generated by micromoulding in capillaries (34) or microlithographic procedures using deep ultraviolet laser irradiation (35, 36).

Biochemistry, Genetics, and Structure

Since the early days of S-layer research, biochemical methods, including sodium dodecyl sulfate polyacrylamide gel electrophoresis (SDS-PAGE) and amino acid analysis, combined with data from electron microscopical investigations, have provided basic knowledge on ultrastructure and chemical composition of archaeal and bacterial S-layer proteins (for reviews see Refs (1, 7, 15, 25, 37–39)). Nowadays, these information can be refined with data from atomic force microscopy (AFM) and other biochemical and biophysical investigations using, for instance, surface plasmon resonance (SPR) spectroscopy, quartz crystal microbalance with dissipation monitoring (QCM-D), and X-ray diffraction analyses of three-dimensional (3-D) crystals.

From initial SDS-PAGE analyses, information about the apparent molecular masses of the constituting SDS-soluble S-layer protomers and their purity and homogeneity can be derived. It has been demonstrated that most S-layers are composed of single, high molecular mass polypeptide species with apparent molecular masses of 40–20 kDa, which, in some cases, are glycosylated (for reviews see Refs (12, 37, 38)). For a few strains, it has been convincingly demonstrated that their S-layer is composed of more than one, often immunologically not cross-reactive, S-layer protein (40–45). S-layer proteins are generally weakly acidic proteins with a 40–60% proportion of hydrophobic amino acids and a rather low amount of sulfur-containing amino acids. The isoelectric points of many intact S-layer proteins range from approximately 4 to 6. However, for S-layers of some *Lactobacilli* pI values >9 have been calculated (46). Despite the above-mentioned variations of S-layer proteins, no profound differences in the overall amino acid composition have been observed. In contrast, remarkable differences were determined for the molecular masses of the constituting subunits and the lattice types and lattice dimensions of S-layers (1, 12, 38).

Because of the diversity in the supramolecular structure of prokaryotic cell envelopes, different disruption and isolation procedures for S-layers have been developed. Usually, they are isolated from purified cell wall fragments by the addition of chaotropic agents (e.g. guanidinium hydrochloride or urea) (for review see Refs (47, 48)), detergents, or cation substitution (e.g. Na⁺ or Li⁺ replacing Ca²⁺) (49). Extraction and disintegration experiments revealed that the inter-subunit bonds in the S-layer lattice are stronger than those binding the subunits to the supporting cell wall (50). Special isolation procedures are required for S-layers in those archaea in which they are associated with the plasma membrane or other cell envelope structures. For example, the filamentous sheathed methanogen, *Methanospirillum hungatei*, synthesizes unusual extracellular crystalline macromolecular layers, which have been investigated in great detail by Beveridge and coworkers in the past decade. The bacteria are encased in a filamentous sheath of unusual stability (51). Neither an alkali dissolution technique nor a combined treatment using sodium dodecyl sulfate (SDS) and β -mercaptoethanol or even 90% phenol proved very effective to produce distinct solubilized sheath components (52). A comparable chemical stability has been observed with the S-layer protein of *Thermoproteus tenax* (53) and other archaeal S-layers (54).

Since the amino acid sequence of an S-layer protein does not provide any information on the location of individual amino acid residues in an S-layer protein, the topology of the S-layer protein of *Geobacillus stearothermophilus* PV72/p2 (SbsB) was investigated (55). Twenty-three single cysteine mutants, which were previously mapped to the surface of the SbsB monomer (55), were subjected to a cross-linking screen using the photoactivatable, sulfhydryl-reactive reagent *N*-[4-(*p*-azidosalicylamido)butyl]-3-*ap*os-(2-*ap*os-pyridyldithio)propionamide. Gel electrophoretic analysis to identify cross-linked dimers indicated that 8 out of 23 residues were located at the interface of the SbsB subunits. In combination with surface accessibility data for the assembled protein, 10 residues were assigned to positions at the inner, cell wall-facing lattice surface, while 5 residues were mapped to the outer, ambient-exposed lattice surface. In addition, the cross-linking screen identified six positions of intramolecular cross-linking within the assembled protein, but not in the monomeric S-layer protein (55). The results are an important step toward the further elucidation of the 3-D structure of the S-layer protein via, for example, X-ray crystallography and cryoelectron microscopy.

Predictions about the secondary structure of different S-layer proteins (e.g. *Aeromonas salmonicida*, *Campylobacter fetus*, and *G. stearothermophilus*) have been derived from comparisons of circular dichroism (CD) spectra under native and denaturing conditions (56–58). The SbsB was dissected into an N-terminal part defined by the three consecutive S-layer homologous (SLH) motifs and the remaining large C-terminal part. Both parts of mature SbsB were produced as separate recombinant proteins (rSbsB_{1–178} and rSbsB_{177–889}) and compared with the full-length form rSbsB_{1–889} (rSbsB). Evidence for functional and structural integrity of the two truncated

4 NANOTECHNOLOGICAL APPLICATIONS OF S-LAYERS

forms was provided by optical spectroscopic methods and electron microscopy. In particular, binding of the SCWP [for details see (59)] revealed a high affinity dissociation constant of 3 nM and could be assigned to the soluble rSbsB₁₋₁₇₈, whereas rSbsB₁₇₇₋₈₈₉ self-assembled into the same lattice as the full-length protein. Furthermore, thermal as well as guanidinium hydrochloride-induced equilibrium unfolding profiles monitored by intrinsic fluorescence and CD spectroscopy allowed characterization of rSbsB₁₋₁₇₈ as an α -helical protein. The C-terminal form rSbsB₁₇₇₋₈₈₉ could be characterized as a β -sheet protein with typical multidomain unfolding. Both truncated forms together showed identical properties with respect to structure and function when compared with the full-length rSbsB. Consequently, rSbsB is characterized by its two functionally and structurally separated parts, the specific SCWP-binding domain rSbsB₁₋₁₇₈ and the larger domain rSbsB₁₇₇₋₈₈₉ responsible for formation of the crystalline array (58).

Although considerable knowledge has been experimentally accumulated on the structure, biochemistry, and assembly characteristics of S-layer proteins, no structural model at atomic resolution is available so far. Recently, the first tertiary structure prediction for SbsB was published (60). The calculation was based on the amino acid sequence of SbsB by performing molecular dynamic simulations using the mean force method. The obtained tertiary structure of SbsB led to a thermodynamically favorable atomic model for this S-layer protein. According to data base comparisons, the primary sequence of SbsB does not have significant similarity to other proteins with known tertiary structure, whereas, as per the calculation, there are similarities to other S-layer proteins, especially concerning the N-terminal region (aa 1-aa 207), which leads to the assumption that there are conserved domains within the S-layer protein family (60).

S-layer proteins of the investigated bacilli possess the intrinsic property to rapidly form two-dimensional (2-D), regularly ordered protein crystals, preventing the formation of 3-D crystals suitable for X-ray diffraction analysis (15, 61). After the S-layer protein gene *sbsC* from *G. stearothermophilus* ATCC 12980^T has been sequenced, the corresponding S-layer protein SbsC (S-layer protein of *G. stearothermophilus* ATCC 12980) was the first one for which different N- or C-terminally truncated S-layer protein forms were recombinantly produced and systematically surveyed for their self-assembling and recrystallization properties (62). It turned out that distinct N- or C-terminally truncated forms of SbsC were water soluble, and, thus, well suited for first three-dimensional 3-D crystallization studies. From the C-terminally truncated form rSbsC₃₁₋₈₄₄, crystals could be obtained, which diffracted to a resolution of 3 Å (63). Native and heavy atom derivative data confirmed the results of the secondary structure prediction, which indicated that the N-terminal region comprising the first 257 amino acids is mainly organized as α -helices, whereas the middle and C-terminal part of SbsC consist of loops and β -sheets. In a very recent study, refinement of preliminary data led to the first high resolution structure (2.4 Å resolution) of the soluble N-terminal form rSbsC₃₁₋₈₄₄ (64). The crystal structure of rSbsC₃₁₋₈₄₄

revealed a novel fold, consisting of six separate domains, which are connected by short flexible linkers. Furthermore, SCWP binding induced considerable stabilization of the N-terminal domain (64).

Recently, the basic mechanism for anchoring an S-layer protein devoid of SLH motifs to the rigid cell wall layer was systematically investigated by SPR biosensor technology using SbsC and the corresponding nonpyruvylated SCWP of *G. stearothermophilus* ATCC 12980^T as the model system (65). Two C-terminal truncations of SbsC (rSbsC₃₁₋₂₇₀ and rSbsC₃₁₋₄₄₃) carrying the SCWP-binding domain as well as one N-terminal truncation (rSbsC₆₃₈₋₁₀₉₉) comprising the residual part of SbsC were recombinantly produced and used for binding studies with peptidoglycan-containing sacculi and evaluation by SDS-PAGE as well as by SPR studies. The SPR data from the complementary experimental setups, in which either the truncated rSbsC forms or the SCWPs were immobilized on the sensor surface, confirmed that the N-terminal region comprising the amino acid residues 31-270 was exclusively responsible for SCWP binding. Analysis of the data from the different setups revealed binding constants (K_d) between 9.32×10^{-5} and 2.05×10^{-12} M affinity, depending on the reaction conditions (65).

In this context, it is interesting to note that in different organisms different SCWPs have been found, all linking the S-layer protein to muramic acid residues of the underlying peptidoglycan sacculus (59). There is one group of SCWPs that possesses a backbone structure of disaccharide repeats— $[\beta$ -D-ManpNAc-(1→4)- β -D-GlcpNAc-(1→3)]_n—with different substituents on the ManNAc residues. Another SCWP group has the tetrasaccharide backbone structure— $[\beta$ -D-ManpNAc3NAcA-(1→6)- α -D-Glcp-(1→4)- β -D-ManpNAc3NAcA-(1→3)- α -D-GlcpNAc-(1→)]_n—with changing modification of the carboxyl groups, whereas in the third group, the structure is completely unrelated to the other two groups (for details see Ref. 66). Owing to the fact that SCWPs are either charged (e.g. by pyruvylation or uronic acids with free carboxyl groups) or noncharged (e.g. neutral glycans or uronic acids with modified carboxyl groups), different binding mechanisms of the respective S-layer proteins must exist in the individual organisms.

Concerning chemical modification of S-layer proteins, glycosylation (37, 39, 54, 67–70) and phosphorylation (71) have been found, with the former, rather complex modification being the most frequent one. S-layers were the first prokaryotic glycoproteins described (72, 73). Of particular interest is that many S-layer glycan chains consist of repeating units that resemble O-antigens of lipopolysaccharides of gram-negative eubacteria (74). Recent analyses of linkage regions of S-layer glycoproteins have shown not only the occurrence of both well known but also completely new linkage types such as the N-glycosidic linkage glucose→asparagine and the O-glycosidic linkages galactose→tyrosine or galactose→serine/threonine (all sugars in β -linkage) (for details see Ref. 75). Owing to the still limited knowledge about archaeal and bacterial S-layer glycoprotein glycan structures, even now generalizations are still rather difficult. One conclusion, however, is that in bacteria, apparently O-linked long-chain glycans

dominate, whereas in archaea, N-glycosidically linked short heterosaccharides seem to be the preponderant glycan species.

Among archaea, detailed analyses on S-layer glycoproteins have been performed only on the halophiles, *Halobacterium salinarum* (67, 72) and *Haloferax volcanii* (69, 76), and the methanogen, *Methanothermobacter ferredoxinus* (77). Recently, when the flagellum of *Methanococcus voltae* was investigated, it was found that the flagellin proteins possess a total of 15 potential N-linked sequons and show a mass shift by SDS-PAGE indicating significant posttranslational modification. A novel glycan structure elucidated by nuclear magnetic resonance (NMR) analysis was shown to be a trisaccharide composed of β -D-ManpNAcA6Thr-(1 \rightarrow 4)- β -D-GlcpNAc3NAcA-(1 \rightarrow 3)- β -D-GlcpNAc linked to Asn. In addition, the same trisaccharide was identified on a tryptic peptide of the S-layer protein from this organism implicating a common N-linked glycosylation pathway for the surface components, flagella and S-layers (78). Studies on the S-layer glycoprotein of *H. volcanii* showed that in addition to glucose (76), additional sugars are involved in N-glycosylation and assembly of this S-layer protein (79). Mass spectrometry (MS) revealed a pentasaccharide comprising two hexoses, two hexuronic acids, and an additional 190-Da saccharide of yet unknown composition. In AglD-lacking cells (AglD is a specific glycosyltransferase), the S-layer revealed a changed architecture when compared with the wild-type strain, and, in addition, its protease susceptibility was different from that of the wild-type strain. Thus, these experiments showed that N-glycosylation endows *H. volcanii* with the ability to maintain an intact and stable cell envelope in hypersaline surroundings, ensuring survival in this extreme environment (79).

Among bacteria, the best investigated bacterial S-layer glycoprotein is that of the gram-positive, moderately thermophilic organism *G. stearothermophilus* NRS 2004/3a (23, 53, 70, 80–85). To the SgsE (S-layer protein of *G. stearothermophilus* NRS 2004/3a), which consists of 903 amino acids, S-layer glycans are attached via O-glycosidic linkages to different serine and threonine residues of the S-layer protein subunits (80). NMR spectroscopy revealed that the S-layer glycan chains are composed of, on average, 14 trisaccharide repeats with the structure $[\rightarrow 2)\text{-}\alpha\text{-L-Rhap-(1}\rightarrow 3)\text{-}\beta\text{-L-Rhap-(1}\rightarrow 2)\text{-}\alpha\text{-L-Rhap-(1}\rightarrow 3)]_n$, with the terminal repeat being modified by a 2-O-methyl group (80, 86). The glycan chains are bound via an adaptor saccharide of, on average, two α 1,3-linked L-Rhap residues to the hydroxyl group at carbon 3 of a β -D-galactose residue. On SDS-PAGE, a purified S-layer glycoprotein preparation separated into four bands appear, three of which are glycosylated. Straightforward MS methods allowed the accurate determination of the average masses of the three inherently heterogenic glycoprotein species of SgsE to be 101.66, 108.68, and 115.73 kDa, corresponding to SgsE with different numbers of attached glycan chains (83). Each of the glycoforms revealed nanoheterogeneity with variation between 12 and 18 trisaccharide repeats and the possibility of extension of the already known di-rhamnose core region by one additional rhamnose residue (83). On the 93-kDa SgsE S-layer protein, three glycosylation sites

could be unequivocally identified, namely, at position threonine₅₉₀, threonine₆₂₀, and serine₇₉₄. These data led to the interpretation that in the 101.66-kDa glycoform only one glycosylation site is occupied, in the 108.68-kDa glycoform two, and in the 115.73-kDa glycoform all three glycosylation sites are occupied (83).

In the course of the genetic characterization of the *G. stearothermophilus* NRS 2004/3a S-layer protein glycosylation, \sim 16.5-kb surface layer glycan biosynthesis (*slg*) gene cluster has been sequenced (GenBank AF328862) (81, 82). The cluster is located immediately downstream of the S-layer structural gene *sgsE* and consists of 13 ORFs that have been identified by database sequence comparisons. There is evidence that the *slg* gene cluster is transcribed as a polycistronic unit, whereas *sgsE* is transcribed monocistronically (82). In addition to *G. stearothermophilus* NRS 2004/3a, the complete *slg* gene clusters of *Aneurinibacillus thermoaerophilus*, strains L420-91^T and DSM 10155 (GenBank AY442352 and AF324836, respectively) and the incomplete cluster of *Thermoanaerobacterium thermosaccharolyticum* E207-71 (GenBank AY422724) are known (81). The genetic organization of the chromosomal *slg* gene clusters of all investigated strains is comparable (68, 70). In addition, the glycan structures of these and several other investigated S-layer glycoproteins are summarized in (4, 68, 75).

The chemical characterization and knowledge of the structure of the different S-layer (glyco)proteins as well as of the underlying molecular machinery are the essential basis for a successful nanotechnological application of these supramolecular cell surface molecules.

During the last decade, sequence data on S-layer genes from organisms of quite different taxonomic affiliations have accumulated. In a recent review, these informations are summarized since 1995 (for older references see Refs (4, 38, 87)) including a complete coverage of GenBank accession numbers of S-layer structural genes and presently known data on surface layer glycosylation (*slg*) gene clusters (16).

Especially for pathogenic organisms such as *Bacillus anthracis*, *Clostridium difficile*, and *C. fetus*, for which specific identification and discrimination are vital for the accurate treatment of afflicted persons, the S-layer gene sequence turned out to be a valuable tool. In this context, S-layer sequence typing (alone or in combination with other typing methods) was found to be a rapid and reproducible alternative especially when specimens contain only small numbers of cells or are inappropriate for culturing (88–92).

Since cell surface components can generally be considered as nonconservative structures that determine the interaction between the living cell and its environment, the observation of phenotypic S-layer variation was not surprising. S-layer variation has been described to occur in pathogens as well as in nonpathogens and leads to the synthesis of alternate S-layer proteins, either by the expression of complete (silent) S-layer genes or by recombination of partial coding sequences (93–102).

Variant formation upon prolonged cultivation under nonoxygen limited conditions was investigated in detail for *G. stearothermophilus* PV72/p6, whose hexagonal S-layer

6 NANOBIOLOGICAL APPLICATIONS OF S-LAYERS

lattice formed by SbsA was replaced by an oblique lattice consisting of the SbsB (96). On the molecular biological level, variant formation was found to depend on recombinational events between a megaplasmid and the chromosome (103).

To conclude, multiple mechanisms leading to S-layer protein variation, modification, or even complete loss of the S-layer indicate the importance of diversification of the surface properties even of closely related organisms for their survival in a competitive habitat.

Anchoring of S-Layer Proteins to the Bacterial Cell Wall

Although sequence comparison of S-layer genes from different archaea and bacteria have revealed that identities between taxonomically unrelated organisms are low, at least for S-layer proteins of gram-positive bacteria, common structural organization principles have been identified. In this context, a cell wall targeting domain was found either at the N-terminal or C-terminal region of S-layer proteins. Concerning N-terminal cell wall targeting, three repeats of SLH motifs, consisting of 50–60 amino acids each, have been identified at the N-terminus of many S-layer proteins (104). Results obtained in a recent study indicated that the highly conserved TRAE motif has a key role in the binding function of SLH domains (105). If present, SLH motifs are involved in cell wall anchoring of S-layer proteins by recognizing a distinct type of heteropolysaccharide, termed SCWP, embedded in the peptidoglycan layer (58, 106–115). The highly specific lectin-type binding between S-layer proteins and SCWPs is an important mechanism for generating and maintaining a dynamic protein crystal on a bacterial cell surface during all stages of cell growth and division (4).

For SLH-mediated binding, the construction of knock-out mutants in *B. anthracis* and *Thermus thermophilus* in which the gene encoding a putative pyruvyl transferase was deleted demonstrated that the addition of pyruvic acid residues to the peptidoglycan-associated cell wall polymer was a necessary modification (111, 113). Recently, the structure of the major cell wall polysaccharide from *B. anthracis* was determined (116). The composition of the polysaccharide was reported to be Gal, ManNAc, and GlcNAc in a 3:1:2 molar ratio. Strong evidence for glycan pyruvylation was also provided by SPR spectroscopy measurements for which the SbsB and the corresponding SCWP, whose structure could be resolved by NMR recently (117), were used for interaction studies (114). The SLH domain of SbsB (rSbsB_{32–208}) was found to be exclusively responsible for SCWP binding, whereas the larger C-terminal part represents the self-assembly domain (58, 114). In contrast to SbsB, in SbpA, the S-layer protein of *L. sphaericus* CCM 2177 (formerly *Bacillus sphaericus*), the three SLH motifs and an additional 58 amino acids long SLH-like motif located behind the third SLH motif were required for reconstituting the functional SCWP-binding domain (115, 118).

A further type of binding mechanism between S-layer proteins and SCWPs has been described for *G. stearothermophilus* wild-type strains, which involves a nonpyruvylated SCWP containing 2,3-diacetamido-2,3-

dideoxymannuronic acid as the negatively charged component and a highly conserved N-terminal region lacking an SLH domain (80, 119, 120). In these S-layer proteins, arginine and tyrosine, which typically occur in carbohydrate-binding proteins such as lectins, are accumulated in the N-terminal part (121). Different N- or C-terminally truncated forms of SbsC were produced and used for elucidation of the structure–function relationship (62), for interaction studies with the corresponding SCWP by SPR biosensor technology (65) as well as for 3-D crystallization studies of this S-layer protein (63, 64) (see also Section titled Biochemistry, Genetics and Structure).

In the case of *Lactobacillus* S-layer proteins, SLH motifs have not been found either; yet, the attachment of the S-layer protein to the cell wall seems to involve also SCWPs in several *Lactobacilli* (122). The S-layer proteins from *Lactobacillus brevis* and *Lactobacillus buchneri* are reported to bind to a neutral polysaccharide moiety of the cell wall, but the location of the cell wall-binding domain of these proteins is currently unknown. On the other hand, the location of the cell wall-binding domain in SlpA of *Lactobacillus acidophilus* ATCC 4356 and CbsA of *Lactobacillus crispatus* JCM 5810 has been determined to reside in the C-terminal one third of these S-layer proteins and sequence alignment studies revealed a putative carbohydrate-binding repeat comprising approximately the last 130 C-terminal amino acids, which were suggested to be involved in cell wall binding (123, 124).

In contrast to gram-positive bacteria, no general S-layer anchoring motifs have been identified in gram-negative organisms. In a recent study using reattachment assays, the anchoring region of the S-layer protein RsaA from *Caulobacter vibrioides* was found to lie in the N-terminal region comprising approximately the first 225 amino acids (125).

To conclude, nature has developed more than one solution to allow the maintenance of a monomolecular closed protein lattice that represents the simplest type of membranes developed during biological evolution (1, 11). The SCWP-mediated anchoring of S-layer subunits to the rigid cell wall layer has high biological relevance since it guarantees a defined orientation and incorporation of the S-layer protein upon reaching the cell surface while allowing enough flexibility for recrystallization of S-layer subunits to continuously assume a low free energy arrangement during cell growth and cell division.

RECOMBINANT S-LAYER FUSION PROTEINS

Construction Principles

For nanobiotechnological utilization of self-assembly systems, S-layer technology was advanced by the construction of genetically engineered S-layer fusion proteins that comprised (i) the N-terminal cell wall anchoring domain, (ii) the self-assembly domain, and (iii) a functional sequence (7, 8, 126). Owing to this construction principle, the functional sequences are aligned at a predefined distance in the nanometer range on the outermost surface of the S-layer lattice, and thus remain available for further binding reactions (e.g. substrate binding and antibody

binding). Concerning the introduction of specific functions, the advantages offered by the S-layer self-assembly system are (i) the requirement of only a simple, one-step incubation process for site-directed immobilization without preceding surface activation of the support, (ii) the general applicability of the "S-layer tag" to any functionality, and (iii) the provision of a cushion to the functional group through the S-layer moiety of the fusion protein preventing denaturation, and, consequently, loss of reactivity upon immobilization.

SbpA consists of 1268 amino acids, including a 30-amino acid-long signal peptide (118). By producing various C-terminally truncated forms and performing surface accessibility screens, it became apparent that amino acid position 1068 is located on the outer surface of the square lattice and that this C-terminally truncated form fully retained the ability to self-assemble into a square S-layer lattice with a center-to-center spacing of the tetrameric morphological units of 13.1 nm (118). Therefore, the C-terminally truncated form rSbpA₃₁₋₁₀₆₈ was used as base form for the construction of various S-layer fusion proteins. An advantage of the SbpA system for nanobiotechnological applications is, that the recrystallization is dependent on the presence of calcium ions, thus allowing control over lattice formation (127).

SbsB consists, in total, of 920 amino acids, including a 31-amino acid-long signal peptide (128). As the removal of 15 amino acids from the C-terminus led to water-soluble rSbsB forms, the C-terminal part can be considered extremely sensitive against deletions. When the C-terminal end of full-length SbsB was exploited for linking a foreign functional sequence, water-soluble S-layer fusion proteins were obtained (129), which recrystallized into the oblique (p1) lattice on a great variety of solid supports. For some specific applications, functional groups were fused toward the N-terminus of SbsB to construct self-assembling S-layer fusion proteins, which attached with their outer surface to, for example, liposomes and silicon wafers, so that the N-terminal region with the fused functional sequence remained exposed to the environment (129).

The protein precursor of SbsC includes a 30-amino acid-long signal peptide and consists of 1099 amino acids (120). The investigation of the self-assembling properties of several truncated SbsC forms revealed that 179 amino acids could be deleted from the C-terminal part without interfering with the self-assembling property of the S-layer protein (62). Thus, SbsC₃₁₋₉₂₀, the shortest C-terminal truncation still capable of forming self-assembly products, was used as base form for the construction of a functional SbsC fusion protein (130).

SgsE is a 903-amino acid protein, including a leader sequence of 30 amino acids. The mature S-layer protein has a calculated molecular mass of 93.7 kDa and an isoelectric point of 6.1 (80). Naturally, SgsE monomers are aligned into a two-dimensional crystalline array with oblique symmetry (lattice parameters, $a = 11.6$ nm, $b = 9.4$ nm, $\gamma \sim 78^\circ$ (80, 131). In the SgsE nanolattice, one morphological unit corresponds to an SgsE dimer, and between the constituent monomers, pores of identical shape are present. Deleting 130 or 330 amino acids

from the N-terminus of SgsE does not influence S-layer self-assembly. Self-assembly products typically appear in the form of flat sheets and double-layered cylinders with diameters decreasing with progressing truncation. All forms of rSgsE are able to recrystallize as a closed, monomolecular protein layer suspension, on negatively charged, unilamellar liposomes and on planar supports. Comparison of the spatial accessibility of the S-layer protein termini by electron microscopic investigation of immuno-gold labeled preparations of hexahistidine-tagged SgsE self-assembly proteins indicated that the C-terminus was more surface exposed, while the N-terminus seemed to be buried within the protein mass. On the basis of these data, the C-terminus of rSgsE was selected as fusion site for the biocatalytic function (132).

Functionalization by Incorporation of Biologically Active Sequences

A great variety of functional S-layer fusion proteins was cloned and heterologously expressed in *Escherichia coli* (Table 1 and Fig. 4). The S-layer fusion proteins based on SbsB, SbsC, SbpA, and SgsE incorporate the Fc-binding domain (ZZ) of protein A (Fig. 4a), the major birch pollen allergen (Bet v1) (Fig. 4b), a hypervariable region of a heavy chain camel antibody (cAb) (Fig. 4c), core streptavidin, the enhanced green fluorescent protein (EGFP) (Fig. 5), metal-binding peptides, enzymes, or a virus epitope, and were successfully produced by recombinant technologies and recrystallized on various solid supports, for example, gold chips, silicon wafers, polystyrene beads, or on liposomes. Owing to the high density and regular display of the introduced functions, a broad range of applications of S-layer fusion proteins has been envisaged, particularly in the fields of biotechnology, molecular nanotechnology, and biomimetics (Table 2) (6–8, 10).

Owing to the versatile applications of the streptavidin (STV)–biotin interaction as a biomolecular coupling system, minimum-sized core STV was either fused to N-terminal positions of the SbsB or to the C-terminal end of the truncated form SbpA₃₁₋₁₀₆₈ (Fig. 4d and Fig. 6) (129, 133, 138). Functional heterotetramers were obtained by mixing an excess of core STV with the fusion proteins, followed by a protein refolding procedure. Analysis of negatively stained preparations of self-assembly products formed by these S-layer fusion proteins revealed that neither the oblique S-layer lattice of SbsB nor the square lattice of SbpA had changed due to the presence of the fusion partner (Fig. 6b and c). Hybridization experiments with biotinylated and fluorescently labeled oligonucleotides using SPR spectroscopy indicated that a functional sensor surface could be generated by recrystallization of heterotetramers on gold chips (Fig. 4d), which has a broad range of potential applications in (nano)biotechnology (133, 138).

The two chimeric S-layer proteins rSbpA₃₁₋₁₀₆₈/Bet v1 and rSbsC₃₁₋₉₂₀/Bet v1 carrying the major birch allergen Bet v1 at the C-terminus maintained both the ability to self-assemble and the functionality of the fused allergen (Fig. 4b) (130, 135). Owing to its immunomodulating capacity, these fusion proteins are generally considered

Table 1. Functional S-Layer Fusion Proteins

S-layer Fusion Protein	Functionality	Length of Functional Domain	Biotechnological Application	Reference
rSbsB ₁₋₈₈₉ /STV	Core streptavidin	118 aa	DNA chips (binding of biotinylated ligands)	129
rSbpA ₃₁₋₁₀₆₈ /STV	Major birch pollen allergen	116 aa	Vaccine development (immunotherapy of type 1 allergy)	133
rSbpA ₃₁₋₁₀₆₈ /Bet v1				130
rSbsC ₃₁₋₉₂₀ /Bet v1	Strep-tag I	9 aa	Affinity tag for streptavidin	118
rSbpA ₃₁₋₁₂₆₈ /STI				118
rSbpA ₃₁₋₁₀₆₈ /STI				
rSbpA ₃₁₋₁₀₆₈ /ZZ	IgG-binding domain	116 aa	High density affinity coating (extracorporeal blood purification)	134
rSbpA ₃₁₋₁₀₆₈ /EGFP	Green fluorescent protein	238 aa	Immune therapy (coating of liposomes for drug delivery)	135
rSbpA ₃₁₋₁₀₆₈ /cAb	Heavy chain camel antibody	117 aa	Protein chips (sensing layers for label-free detection systems)	139
rSbpA ₃₁₋₁₀₆₈ /AG4	Silver-binding peptide	12 aa	Nanoparticle arrays (oriented binding of metal nanoparticles)	Naik and Stone, Personal communication
rSbpA ₃₁₋₁₀₆₈ /AGP35				
rSbpA ₃₁₋₁₀₆₈ /CO2P2	Cobalt-binding peptide	12 aa	Biocatalysts	136
rSbpA ₃₁₋₁₀₆₈ /LamA	(Hyper)thermophilic enzyme	263 aa		
rSgsE ₃₃₁₋₉₀₃ /RmlA	Glucose-1-phosphate thymidyltransferase	299 aa		
rSbpA ₃₁₋₁₀₆₈ /F1	Mimotope, mimicking an immunodominant epitope of Epstein-Barr virus (EBV)	20 aa	EBV diagnostics	137
rSbsB ₁₋₈₈₉ /F1				

^aMature S-layer proteins: SbpA of *Lysinibacillus sphaericus* CCM 2177 (1238 aa); SbsB of *Geobacillus stearothermophilus* PV72/p2 (889 aa); SbsC of *Geobacillus stearothermophilus* ATCC 12980 (1099 aa); and SgsE of *Geobacillus stearothermophilus* NRS 2004/3a (903 aa).

as a novel approach to specific treatment of allergic diseases (e.g. carrier/adjuvant in design of vaccines for immunotherapy of type 1 allergy) (8).

The S-layer fusion protein rSbpA/ZZ (Fig. 4a) incorporates two copies of the ZZ, a synthetic analog of the IgG-binding domain of protein A from *Staphylococcus aureus* (134). On average, ~66% of the theoretical saturation capacity of a planar surface was covered by IgG aligned in upright position. By recrystallization of this chimeric protein on microbeads, novel biocompatible microparticles for the microsphere-based detoxification system were generated, which are extremely promising for their application as immunoadsorbents for extracorporeal blood purification of patients suffering from autoimmune disease (134).

The S-layer fusion protein rSbpA₃₁₋₁₀₆₈/EGFP (Fig. 5) containing EGFP was recrystallized as a monolayer on the surface of positively charged liposomes. Because of its ability to fluoresce, liposomes coated with rSbpA₃₁₋₁₀₆₈/EGFP (Fig. 5c and f) is a useful tool to visualize the uptake of S-layer-coated-liposomes (S-liposomes) into eukaryotic cells (135).

S-layer fusion proteins comprising the C-terminally truncated form rSbpA₃₁₋₁₀₆₈ and the hypervariable region of heavy chain camel antibodies recognizing lysozyme or a PSA (Fig. 4c) were recrystallized as a monolayer on SCWP-coated gold chips and used as sensing layer in biochips for SPR spectroscopy (139, 140).

Another line of development aims at the construction of novel biocatalysts based on fusion proteins between S-layer proteins of *Bacillaceae* and enzymes from extremophiles (Fig. 7), as required for many biotechnological applications (132, 136).

APPLICATION POTENTIAL OF NATIVE AND CHIMERIC S-LAYERS

S-Layers for Nanobiotechnological and Biomimetic Applications

S-Layer Ultrafiltration Membranes. Ultrafiltration is used to retain macromolecules from a solution. The rejection characteristics of ultrafiltration membranes (membranes with pore sizes from 2 to 50 nm) are theoretically determined by the size, shape, and physicochemical properties of the solutes relative to the pore size in the permselective layer (141, 142). Generally, ultrafiltration membranes are produced from a broad spectrum of polymers (e.g. cellulose derivatives and polysulfone ionic polymers) by a phase inversion process. Conventional polymer ultrafiltration membranes possess an amorphous structure and a pore size distribution with pores differing in size by as much as one order of magnitude and a porosity, usually, lower than 10% (141, 142).

Studies on the permeability properties of S-layers from various *Bacillaceae* revealed that these monomolecular

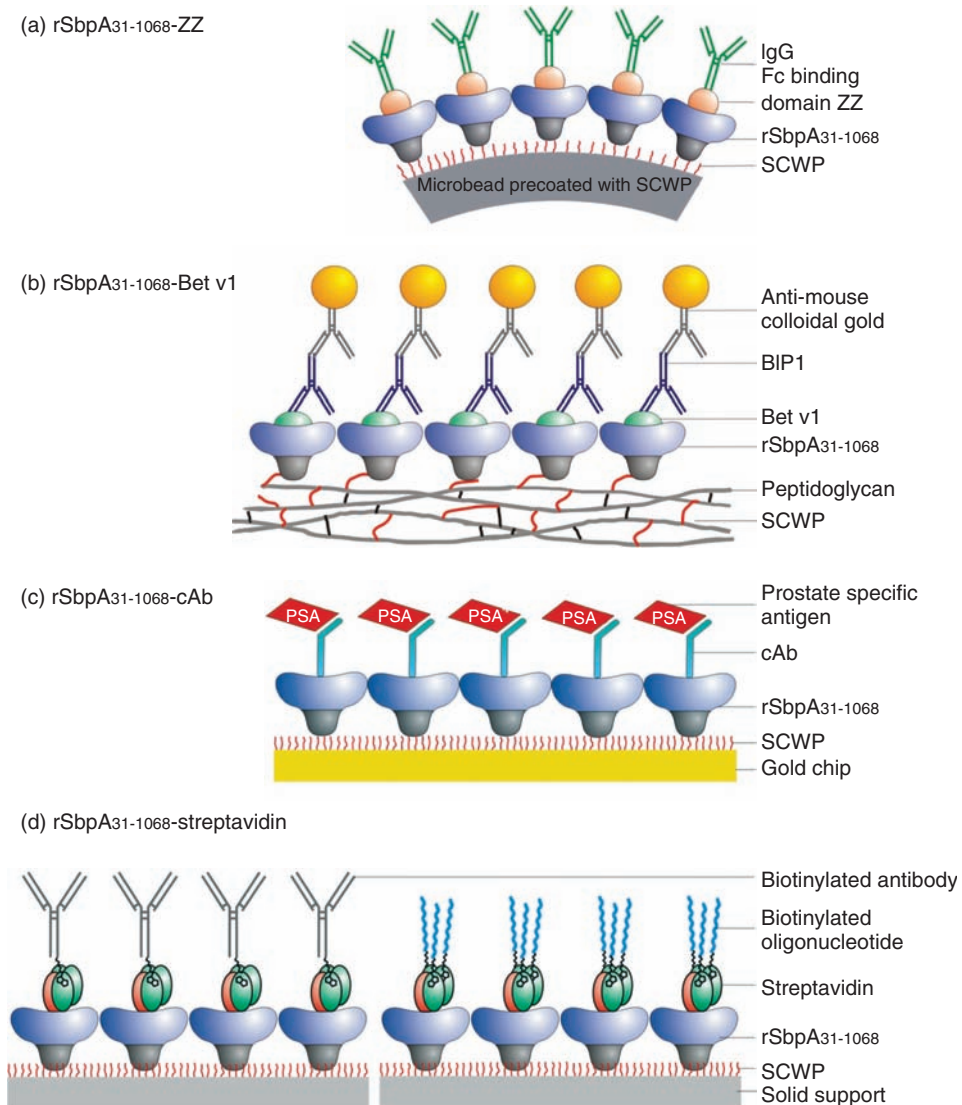


Figure 4. Schematic drawing illustrating detection systems based on C-terminal rSbpA-fusion proteins (for abbreviations see section titled List of Abbreviation). (a) rSbpA₃₁₋₁₀₆₈-ZZ was recrystallized on SCWP-coated microbeads to which human IgGs could bind via the Fc part. (b) rSbpA₃₁₋₁₀₆₈-Bet v1 was recrystallized on peptidoglycan-containing sacculi involving binding to SCWP. The presence of Bet v1 epitopes was checked by immunoreactivity with BIP1, a monoclonal mouse anti-Bet v1 that could be visualized by TEM after incubation with anti-mouse colloidal gold. (c) rSbpA₃₁₋₁₀₆₈-cAb was recrystallized on gold chips precoated with the thiolated SCWP. The monomolecular protein lattice was able to specifically bind prostate-specific antigen (PSA) on the outermost surface. (d) rSbpA₃₁₋₁₀₆₈-streptavidin heterotetramers were recrystallized on gold chips precoated with thiolated SCWP. After recrystallization into a monomolecular protein lattice, biotinylated molecules (proteins or oligonucleotides) were bound.

protein lattices function as molecular sieves within the ultrafiltration range (143–146). Because of the presence of pores of identical size and morphology, S-layers were considered as model systems for producing isoporous ultrafiltration membranes for the first time. S-layer ultrafiltration membranes (SUMs) are made by depositing either S-layer self-assembly products or S-layer-carrying cell wall fragments on conventional microfiltration membranes with a pore size of approximately $0.5\ \mu\text{m}$ in a pressure-dependent procedure (147).

The concentration of the S-layer carrying cell wall fragments was adjusted in a way that a coherent layer was generated on the surface of the microporous support. After deposition, S-layer fragments can be cross-linked, preferentially with glutaraldehyde. To increase the chemical stability of cross-linked S-layer lattices, Schiff bases formed by the reaction of glutaraldehyde with ϵ -amino groups from lysine were reduced with sodium borohydride (148). SUMs produced of S-layer carrying cell wall fragments from different *G. stearothermophilus* strains exhibited identical exclusion limits as determined for native

and glutaraldehyde-treated S-layer vesicles by applying the space technique (143, 149). The very sharp molecular mass cutoff of SUMs clearly demonstrated that S-layer protein lattices work as isoporous molecular sieves. Comparison to the S-layer lattices from *G. stearothermophilus* strains, the S-layer lattices from *Ly. sphaericus* and *Bacillus coagulans* exhibited cutoff levels shifted slightly to the lower molecular mass range (150, 151). SUMs produced of these S-layer lattices allowed free passage for myoglobin (M_r 17,000) and rejected carbonic anhydrases (M_r 30,000) (Table 3), whereas SUMs made with S-layers from *G. stearothermophilus* strains rejected only carbonic anhydrase to approximately 10% while ovalbumine with a molecular weight of 43,000 was rejected to at least 90%. Cross-linking the S-layer protein with glutaraldehyde during the production of the SUMs led to net negatively charged membranes owing to the reaction of a considerable proportion of free amino groups. Since under physiological conditions the majority of S-layer proteins in solution are negatively charged, it is advantageous for many ultrafiltration processes to use membranes

10 NANOBIOLOGICAL APPLICATIONS OF S-LAYERS

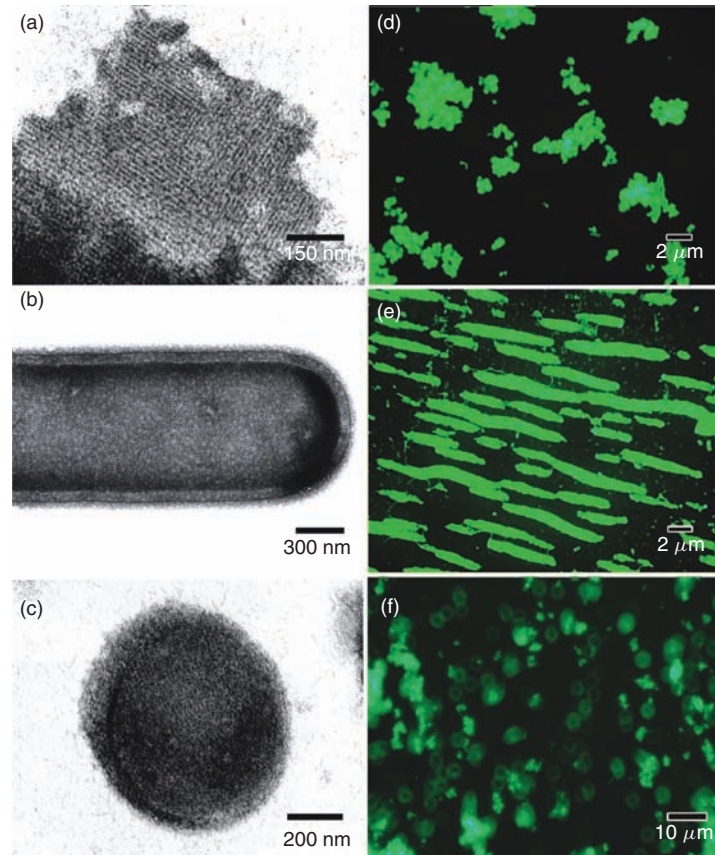


Figure 5. (a)–(c) Electron micrographs of negatively stained preparations. (d)–(f) Fluorescence micrographs of self-assembly products formed by rSbpA/EGFP (a and d), rSbpA/EGFP recrystallized on SCWP containing peptidoglycan-containing sacculi of *Ly. sphaericus* CCM 2177 (b and e), and liposomes coated with the fusion protein rSbpA/EGFP (c and f).

that have a net negative charge. Consequently, SUMs with a net negative surface charge showed no or negligible flux losses after filtration of solutions of ferritin, bovine serum albumin, or ovalbumin, which had a net negative surface charge under the applied experimental conditions (152). Since S-layers are monomolecular arrays of identical (glyco)protein lattices, functional groups (e.g. amino and carboxyl groups) are regularly arranged and exhibit identical positions and orientations on the individual constituent subunits. These repetitive well-defined surface properties allow chemical modifications of SUMs in an unsurpassed controlled way to modify adsorption and rejection properties (3, 153, 154). Routinely, carboxyl groups from the S-layer protein layers on SUMs were activated with 1-ethyl-3(3-dimethylaminopropyl) carbodiimide (EDC) and allowed to react with the free amino groups from nucleophiles of different molecular size, structure, charge, and hydrophilicity or hydrophobicity. Such covalent attachment of low molecular weight nucleophiles to the S-layer lattice not only led to alterations of the surface properties and antifouling characteristics but were also responsible for an accurately controlled shift of the rejection curves to lower molecular weight range (3).

To conclude, SUMs are the only ultrafiltration membranes that allow most accurately controlled modifications of the physicochemical and molecular sieving properties. This broad range of potential modifications allows the properties of SUMs to be adapted to very specific process requirements (3, 143, 155).

Table 2. Areas of Application of S-Layer Fusion Proteins

Diagnostic systems and label-free detections system (sensing layers for surface plasmon resonance spectroscopy, surface acoustic wave, quartz crystal microbalance with dissipation monitoring)
Biosensors
High density affinity coatings (e.g. biocatalysis and immobilized enzymes, downstream-processing, and blood purification)
Immunogenic and immunomodulating structures (e.g. anti-allergic vaccines)
Stabilization of functional lipid membranes
Drug targeting and delivery systems (functionalization of liposomes and emulsomes)
Binding of nanoparticles (e.g. molecular electronics, nonlinear optics, and catalysts)
Biomineralization
Isoporous ultrafiltration membranes

S-Layer-Based Enzyme Immobilization. Different covalent immobilization studies on S-layer lattices showed that regarding the binding density, retained activity, and biospecificity, the optimal activation method is strongly dependent on the respective enzyme, antibody, or ligand (153, 156–158). The enzymes were either coupled to the hexagonally ordered S-layer lattices from *Thermoanaerobacter thermohydrosulfuricus* L111-69 (159) or *G. stearothermophilus* PV72 (160). The covalently bound carbohydrate chains of the S-layer glycoprotein

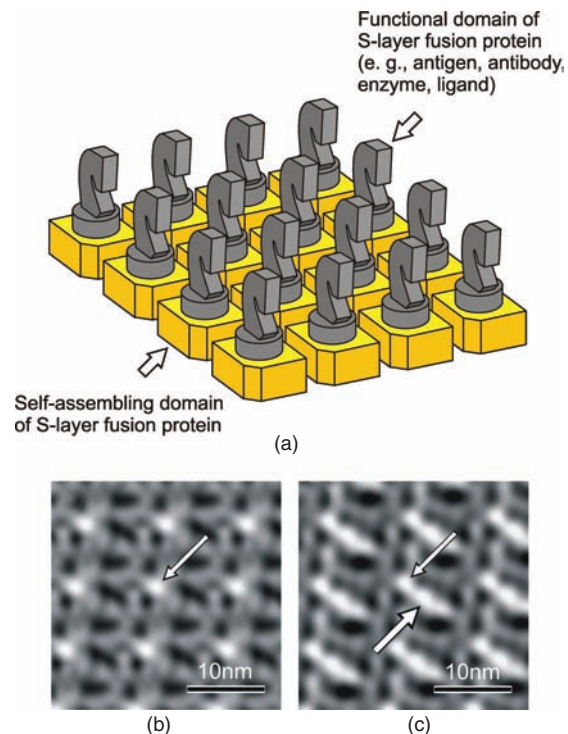


Figure 6. (a) Schematic illustration of the self-assembling parts of S-layer fusion proteins and their well-oriented functional domains. Such arrays theoretically provide the highest possible order (spatial control, orientation, and position) of functional domains at the nanometer level. The knights reassemble the functional domains (antigens, enzymes, antibodies, ligands, etc.) and the cut squares represent the S-layer. Digital image reconstructions of transmission electron micrographs of negatively stained preparations of (b) the native S-layer protein, SbsB, from *G. stearothermophilus* PV72/p2 for which the N-terminal SLH domain is indicated by a thin arrow and (c) S-layer (SbsB)-streptavidin heterotetramers. In the lattice formed by the SbsB-streptavidin heterotetramers (c), streptavidin shows up as an additional protein mass (thick arrow) attached to the N-terminal SLH domain (thin arrow).

from *Th. thermohydrosulfuricus* L111-69 (161, 162) were also exploited for enzyme immobilization (153, 156, 158, 163). The large enzymes, such as invertase ($M_r = 270,000$), glucose oxidase ($M_r = 150,000$), glucuronidase ($M_r = 280,000$) and β -galactosidase ($M_r = 116,000$), formed a dense monolayer on the outer face of the S-layer lattice from different *Bacillaceae* (87). After direct coupling of the enzymes invertase, glucose oxidase, naringinase ($M_r = 96,000$), and β -glucosidase ($M_r = 66,000$) to the EDC-activated carboxylic acid groups of the S-layer protein from *Th. thermohydrosulfuricus* L111-69, the retained enzymatic activities were in the range of 70%, 35%, 60%, and 16%, respectively. By immobilization via spacer molecules, a significant increase in enzymatic activity could be achieved for glucose oxidase and naringinase with 60% and 80%, respectively. The most striking increase was observed for β -glucosidase, for which immobilization via spacers led to a 10-fold increase in activity to 160%. The significant increase in enzymatic activity indicated that immobilization via spacers most

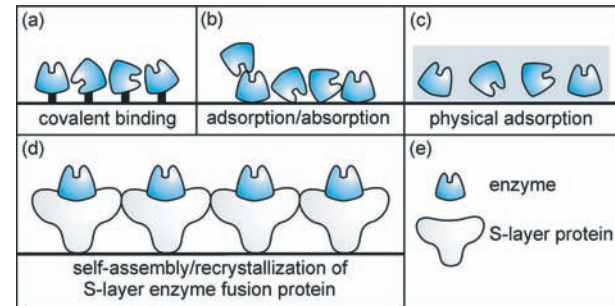


Figure 7. Comparison of different enzyme immobilization methods. (a) Random immobilization via covalent binding; (b) random adsorptive binding; (c) random physical adsorption within a 3-D gel structure; (d) novel approach for site-directed immobilization of an enzyme via the S-layer self-assembling technique, allowing orientated and dense surface display of the enzyme in its native conformation and ensuring accessibility for the substrate.

probably increased the distance between the enzyme molecules and the crystalline S-layer matrix (158).

Current research activities are focused on the production of fusion proteins between S-layer proteins of *Bacillaceae* and enzymes from extremophiles for the development of novel immobilized biocatalysts (Fig. 7) aiming at the controllable display of biocatalytic epitopes, storage stability, and reuse (132, 136) as required for a great variety of application (e.g. biocatalytic processes, diagnostics, chemical-, pharmaceutical-, and food industry).

On the basis of the demonstrated suitability of the S-layer protein self-assembly system for covalent enzyme immobilization (163, 164), a genetic engineering, bottom-up approach was chosen to construct multidomain proteins from a selected, self-assembling portion of an S-layer protein and an enzyme. This concept was exemplified by using two different enzymes. In the first approach, the glucose-1-phosphate thymidyltransferase (RmlA) from *G. stearothermophilus* NRS 2004/3a was C-terminally fused to two truncated forms of the S-layer protein SgsE (SgsE₃₁₋₇₇₃ and SgsE₃₁₋₅₇₃) originating from the same organism (132). Considerable interest in this enzyme originates primarily from its involvement in the biosynthesis of L-rhamnose, which has a confirmed role in pathogenicity of many bacteria (165). In the second approach, a fusion protein comprising the C-terminally truncated form SbpA₃₁₋₁₀₆₈ from *Ly. sphaericus* CCM 2177 and the extremophilic β -1,3-endoglucanase (LamA) from *Pyrococcus furiosus*, which hydrolyzes laminarin-oligosaccharides, was constructed (Fig. 7) (136). Triggered by the intrinsic self-assembling property of the chimeric S-layer-based monomers into an oblique (SgsE) or square (SbpA) 2-D crystalline array with nanometer-scale periodicity, two principal types of S-layer biocatalysts were constructed, namely, (i) self-assembled biocatalysts in solution and (ii) biocatalysts obtained upon recrystallization on diverse supports, such as liposomes, planar glass slides, silicon wafers, and porous polymer membranes. The specific enzyme activity determined for rSbpA/LamA lattices recrystallized as a monolayer on a silicon wafer was 774 U/mg, which matched the specific enzyme activity (727 U/mg) of the native enzyme

Table 3. Rejection Characteristics of SUMs Prepared of S-Layer Carrying Cell Wall Fragments from *Lysinibacillus sphaericus* CCM 2120 [modified after Ref. 3]

Protein	M_r	Molecular size (nm)	pI	% R	pH Value of the Protein Solutions
Ferritin	440,000	12	4.3	100	7.2
Bovine serum albumin (BSA)	67,000	$4.0 \times 4.0 \times 14.0$	4.7	100	7.2
Ovalbumin (OVA)	43,000	4.5	4.6	95	4.6
Carbonic anhydrase (CA)	30,000	$4.1 \times 4.1 \times 4.7$	5.3	80	5.3
Myoglobin (MYO)	17,000	$4.4 \times 4.4 \times 2.5$	6.8	0	6.8

^aThe rejection coefficient (R) was calculated according to the following equation: $R = \ln(C_r/C_0) \ln(V_0/V_r)$. C_r or V_r represents the protein concentration in the retentate or the volume of the retentate; C_0 is the concentration of the protein in the solution before filtration; and V_0 is the initial volume of the feed. The pH value of each protein solution was immediately measured after dissolving the proteins in distilled water.

LamA in aqueous solution (136). Taking the different molecular weights into account, the value given for the fusion protein represents units per milligram calculated to the amount of enzymatic groups. Additional advantage of S-layer-based biocatalysts through provision of a regular display matrix for the enzymatic function was demonstrated after formation of rSbpA/LamA lattices on nonactivated glass slides on which the fusion protein showed a 17-fold higher glucose release per membrane unit area (6.8 mM/cm^2) compared to the native, adhesively immobilized LamA (0.4 mM/cm^2). This finding clearly demonstrates that supports with low binding capacity for an enzyme can be utilized when applying the S-layer fusion protein approach (136). It is conceivable that by using fusion proteins, the S-layer moiety acts as a cushion preventing denaturation of the enzyme moiety upon immobilization (Fig. 7). Furthermore, the S-layer protein portion of the biocatalysts confers significantly improved shelf life to the fused enzyme without loss of activity over more than 3 months, and also enables biocatalyst recycling. In general, clear advantages for enzyme immobilization offered by the S-layer self-assembly system include the high flexibility for variation of enzymatic groups within a single S-layer array by cocrystallization of different enzyme/S-layer fusion proteins to construct multifunctional, nanopatterned biocatalysts, as well as the possibility for deposition of the biocatalysts on different supports with the additional option of cross-linking of individual monomers to improve robustness (136). Especially, liposome-type biocatalysts could make valuable contributions to the fields of nanomedicine, pharmacy, and also nutrition, for which engineering of multifunctional nanocarriers together with the properties such as targetability, longevity, and loading is of high demand (166). Also enzyme immobilization on membranes constitutes an interesting area of applied research, because such microporous composites favor easy flow of substrates and products (167), and may be integrated in more complex processes, in which combination of a catalytic function with a conventional filtration function is required (168). The results obtained in these studies clearly demonstrate that the S-layer-based bottom-up self-assembly systems for functionalizing solid supports with a catalytic function could have significant advantages over processes based on random and covalent immobilization of native enzymes (132, 136).

S-Layers in Diagnostics. SUMs produced of S-layer carrying cell wall fragments from *Ly. sphaericus* CCM 2120 were used for the development of immunoassays and dipsticks (169). By immobilizing monolayers of either protein A or STV onto SUMs, a universal biospecific matrix could be generated (154). Matrices based on protein A as an IgG specific ligand were obtained by immobilizing dense monolayers of this ligand to carbodiimide-activated carboxylic acid groups from the S-layer protein of SUMs (154, 170). Because of the high affinity of human IgG and rabbit IgG to protein A, the protein A-SUM was shown to be particularly suitable for generating dense monolayers of correctly aligned antibodies on the SUM surface. Alternative to protein A, the avidin–biotin or STV–biotin system (171, 172) was applied for SUM-based immunodiagnostic systems. For this purpose, the square S-layer lattice from *Ly. sphaericus* CCM 2120 was cross-linked with glutaraldehyde, and free carboxylic groups were converted into amino groups by modification with ethylenediamine (151). After binding to preactivated biotin, such biotinylated S-layers could adsorb up to 800 ng avidin or STV per square centimeter, which corresponded to a closed monomolecular layer. Mouse IgG with a lower affinity to protein A than human IgG or rabbit IgG was first biotinylated and subsequently bound to such a streptavidin-coated SUM, or alternatively, was directly linked to carbodiimide-activated carboxylic acid groups exposed on the surface of the S-layer lattice (154).

The respective monoclonal antibody was covalently bound to the carbodiimide-activated carboxylic acid groups of the S-layer lattice. Proof of principle was demonstrated for different types of SUM-based dipsticks: For example, for diagnosis of type I allergies (determination of IgE against the Bet v1 in whole blood or serum), for quantification of tissue type plasminogen activator (t-PA) in patients' whole blood or plasma for monitoring t-PA levels in the course of thrombolytic therapies after myocardial infarcts, or for determination of interleukin 8 (IL 8) in supernatants of human umbilical vein endothelial cells (HUVEC) induced with lipopolysaccharides (173–175). Furthermore, a dipstick assay was developed for prion diagnosis based on a sandwich enzyme-linked immuno sorbent assay (ELISA) specific for prion protein, exploiting S-layer lattices as an immobilization matrix. The sensitivity of the prion dipsticks were similar to that published for time-resolved fluorescence ELISA methods, which are among the most sensitive detection methods for prions (176).

Current studies focus on the construction of S-layer fusion proteins comprising antigen functionality and S-layer reassembling properties. The use of peptide epitopes as diagnostic antigens in commercial diagnostics is a promising approach toward simpler and cheaper ELISA-based diagnostic assays. However, because of their small size, peptides are generally weak immunogens on their own. To enhance immunogenicity, S-layer epitope fusion proteins were developed, which combine the ability to form highly ordered protein lattices with a specific antibody-binding affinity. This combination allows direct recrystallization on ELISA plates, thus presenting the peptide sequence in a predictable orientation, freely accessible to antibody binding. The S-layer moiety acts as protein cushion between the solid support and the functional group preventing epitope denaturation, which is a common problem in peptide immobilization. The studies performed with S-layer peptide epitope fusion proteins resulted in an ELISA-based diagnostic assay for serum samples with high sensitivity and specificity, which is applicable to various other peptide epitopes (137).

Another application of S-layers in diagnostics can be seen in the exploitation of S-layer fusion proteins as key elements for the development of sensing layers for label-free detection systems such as SPR, surface acoustic wave (SAW), or QCM-D. In these systems, the specific binding of functional molecules (e.g. proteins or antibodies) to the sensor chip functionalized with an oriented chimeric S-layer can be visualized directly by a mass increase on the chip without the need of any labeled compound. For this purpose, an S-layer fusion protein comprising the C-terminally truncated form rSbpA₃₁₋₁₀₆₈ and the hypervariable region of heavy chain camel antibodies recognizing PSA was recrystallized as a monolayer on SCWP-precoated gold chips and used as sensing layer in biochips for SPR spectroscopy (Fig. 4c). At least three of four possible PSA molecules were bound per morphological unit of the square lattice (140).

S-Layer Stabilized Liposomes and Lipid Membranes. Biological membranes play key roles in cell life, acting as permeability barriers and privileged sites of communication between the inside and outside of cellular worlds (177–180). The current knowledge of the molecular processes occurring at biological membranes is mainly based on studies performed on models of biological membranes, including liposomes and giant vesicles in solution (181, 182), lipid monolayers at the air–water interface (183, 184), black lipid membranes (BLMs) (185, 186), membrane patches at pipettes (187, 188), lipid discs (189, 190), or solid-supported membranes (30, 191–200).

To increase the stability of lipid membranes and to offer many advantages to an experimentalist and for industrial application, several methods like sterically, polymer-, or (nano)particle-stabilized liposomes have been developed (201–205). One promising strategy is the stabilization and functionalization of lipid membranes with S-layer proteins (5, 30, 196, 197, 200). The inspiration for such a composite membrane is the cell envelope structure of gram-negative archaea composed of a plasma membrane, a closely attached or even integrated or penetrating S-layer

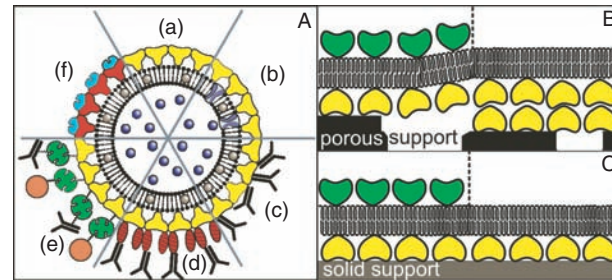


Figure 8. (A) Schematic drawing of an S-layer-coated liposome (S-liposome) with entrapped water-soluble (blue) or lipid-soluble (brown) functional molecules (a) and functionalized by reconstituted integral proteins (b). S-liposomes can be used as immobilization matrix for functional molecules (e.g. IgG) by direct binding (c), immobilization via the Fc-specific ligand protein A (d), or biotinylated ligands can be bound to the S-liposome via the biotin–streptavidin system (e). Alternatively, liposomes can be coated with genetically modified S-layer proteins incorporating functional domains (f). (B) On S-layer ultrafiltration membranes (SUMs), lipid membranes can be generated by a modified Langmuir–Blodgett (LB) technique. As a further option, a closed S-layer lattice can be attached on the external side of the SUM-supported lipid membrane (left part). (C) Solid supports can be covered by a closed S-layer lattice and subsequently lipid membranes can be generated using combinations of the LB- and Langmuir–Schaefer technique, detergent depletion method, and vesicle fusion. Furthermore, a closed S-layer lattice can be recrystallized on the external side of the solid-supported lipid membrane (left part).

lattice, and embedded and integral membrane proteins (25). The S-layer presumably contributes to the remarkable stability of the cell envelope structure as archaea dwell even at most extreme environmental conditions (e.g. 120 °C, pH 0, and concentrated salt solutions) (206, 207). Mimicking this building principle, either membranes composed of artificial or isolated lipid molecules can be stabilized by the closely attached S-layer lattice or on S-layer lattices, membranes with stability and fluidity can be generated (Fig. 8) (25, 30, 193, 196, 200).

Most S-layer subunits are weakly acidic proteins and therefore the S-layer recrystallization process on membranes has been demonstrated to be facilitated by addition of a small portion of positively charged surfactants (e.g. hexadecylamine) (209, 210) or lipid derivatives (211). From this observation, it has been concluded that electrostatic interactions between exposed carboxyl groups on the S-layer lattice (so-called primary binding sites) and the zwitterionic lipid head groups are primarily responsible for the attachment of the S-layer subunits. For such an alignment, it has been suggested that there are at least two to three contact points between the adjacent lipid leaflet and each subunit of the attached S-layer proteins (212). In other words, less than 5% of the lipid molecules are anchored to protein domains on the S-layer lattice, whereas the remaining $\geq 95\%$ lipid molecules of the attached lipid monolayer may diffuse freely into the membrane between pillars consisting of anchored lipid molecules (30, 197). Because of its widely retained fluid characteristic this nanopatterned lipid membrane is also referred to as *semifluid membrane* (213).

Artificial lipid vesicles termed *liposomes* are widely used as delivery systems for enhancing the efficiency of various biological active molecules *in vivo* (181, 182). S-liposomes represent simple model systems resembling features of archaeal cell or virus envelopes (Fig. 8A). The high mechanical and thermal stability of S-liposomes and the possibility for immobilizing or entrapping biologically active molecules (135) reveal a broad application potential, particularly as carrier and/or drug delivery, as artificial virus, and for medicinal applications as drug targeting system or in gene therapy (Fig. 8A) (4, 5, 30, 126, 193, 196, 197, 200, 208, 214). By using S-liposomes carrying a fluorescent monomolecular layer formed by the rSbpA₃₁₋₁₀₆₈/EGFP fusion protein, cell binding and internalization into cell compartments can be followed by confocal laser scanning microscopy (135).

The current interest in reconstituting biological membranes on solid supports aims at linking the biological world, with its elaborate molecular architectures, properties, and functions, to the field of surface science, with its advanced technologies and sophisticated surface-sensitive analytical methods (195, 200). A good deal of studies has demonstrated that S-layers self-assembled on porous (Fig. 8B) and solid supports (Fig. 8C) provide an excellent cushion since the long-term stability and the fluidity of this type of supported lipid membranes are significantly elevated compared to other model membranes (215, 216).

As the ability to manipulate membranes improves, continuing challenges include incorporating and observing complex membrane protein assemblies, device multiplexing, and robustness, as well as device applications. Membrane proteins are key factors in the cell's metabolism, for example in cell-cell interaction, signal transduction, transport of ions and nutrients, and, thus, in health and disease (217). Owing to this important function, membrane proteins are a preferred target for pharmaceuticals [at present more than 60% of consumed drugs (218)] and have received widespread recognition for their application in drug discovery, protein-ligand screening, and biosensors. Thus, it is of utmost importance to generate model membrane systems, for the incorporation of proteins, and membrane-active peptides, to utilize their biological function down to the single functional unit level (178, 180, 214).

Membrane-active peptides-like alamethicin, gramicidin A, or valinomycin have been incorporated in S-layer-supported lipid membranes. In a first study, a tetraetherlipid monolayer was clamped on the tip of a micropipette (tip-dip technique), S-layer proteins were recrystallized on the preformed lipid membrane, and finally valinomycin was incorporated in these S-layer-supported tetraetherlipid monolayers. Interestingly, a 10-fold increase of the life time has been observed for the latter one compared to a tetraetherlipid monolayer without an attached S-layer lattice (219). In a further study, gramicidin A was incorporated into tetraetherlipid monolayers and phospholipid bilayers (Fig. 8B), which have previously been deposited on SUMs (220). These composite membranes revealed not only a remarkable stability, particularly with an S-layer cover, but also the most striking result that

high resolution conductance measurements on single gramicidin pores were feasible. The functionality of lipid membranes resting on S-layer-covered gold electrodes (Fig. 8C) has been demonstrated by the reconstitution of alamethicin, gramicidin A, and valinomycin (221). Owing to the formation of conductive alamethicin channels, the membrane resistance dropped significantly by a factor of ~ 100 , whereas the capacitance was not altered. Partial inhibition of the alamethicin channels with amiloride and analog has been demonstrated as increasing amounts of inhibitor gave rise to an increased membrane resistance. Furthermore, an S-layer-supported lipid membrane with incorporated valinomycin, a potassium-selective ion carrier, revealed a 410-fold lower resistance in potassium buffer than bathed in a sodium buffer (221).

In reconstitution experiments, the pore formation of the staphylococcal α -hemolysin (α HL) (222) has been examined at plain and S-layer-supported lipid membranes (223). α HL has been added to the lipid-exposed side of the S-layer-supported BLM and resulted in pore formation as determined by the increase in conductance. No assembly of α HL has been detected upon adding α HL monomers to the S-layer face of the composite membrane. Therefore, it is concluded that the intrinsic molecular sieving properties of the S-layer lattice did not allow passage of α HL monomers through the S-layer lattice. Compared to plain BLMs, S-layer-supported lipid membranes show a decreased tendency to rupture in the presence of α HL, demonstrating an enhanced stability due to the attached S-layer lattice (223). Most interestingly, even single pore recordings have been performed with α HL reconstituted in S-layer-supported lipid membranes (224) and also with BLMs resting on SUMs (210).

The strategy of the biomimetic approach of copying the supramolecular architecture of archaeal cell envelopes opens new possibilities for exploiting functional lipid membranes at the meso- and macroscopic scale. Moreover, this technology has the potential to initiate a broad range of developments in many areas like sensor technology, diagnostics, targeting, and delivery systems, drug screening devices, (nano)biotechnology, nanomedicine, and electronic or optical devices.

S-Layers for Controlled Immobilization of Nanoparticles.

The chemical synthesis of organized matter represents a new horizon in inorganic materials research. Recent studies have shown that self-assembled organic molecules can be used as preformed or *in situ* templates for controlled deposition of inorganic materials. In particular, the broad base of knowledge about the S-layer-mediated binding of biological molecules has paved the way for investigating the potential of S-layer proteins and their self-assembly products as catalysts, templates, and scaffolds for the generation of ordered nanoparticle arrays for non-life science applications (e.g. nonlinear optics and nanoelectronics).

Several different routes have been described in the literature for fabricating ordered nanoparticle arrays based on S-layers. About two decades ago, S-layer fragments were deposited on solid substrates and subsequently served as micro/nanolithographic mask in a metal evaporation process (225). Although it has been demonstrated that

nanoparticle arrays may be fabricated in this way, the real breakthrough was achieved by using S-layer lattices in the direct precipitation of metals from solution or by binding preformed nanoparticles. In the wet chemical approach, which was derived from the fine grain mineralization from bacteria (226), self-assembled S-layer structures were exposed to metal-salt solutions, such as tetrachloroauric(III) acid (HAuCl_4) solution, followed by slow reaction with a reducing agent such as hydrogen sulfide (H_2S) or by electron irradiation in an electron microscope (227–233). The latter approach is technologically important since it allows the definition of areas where nanoparticles are eventually formed (228, 231). Nanoparticle superlattices were formed according to the lattice spacing and symmetry of the underlying S-layer. Furthermore, since the precipitation of metal ions was confined to the pores of the S-layer, the nanoparticles also resembled the morphology of the pores. The nanoparticles were crystalline, but their ensemble was not crystallographically aligned. Although native S-layers have clearly demonstrated the presence and availability of functional sites for the precipitation of metal ions, a much more controlled and specific way of making highly ordered nanoparticle arrays uses genetic approaches for the construction of chimeric S-layer fusion proteins incorporating unique polypeptides that have demonstrated to be responsible for the *in vitro* formation of inorganic materials (234, 235). The precipitation of metal ions or binding of metal nanoparticles is then confined to specific and precisely localized positions in the S-layer lattice. Currently, several gold, silver, and cobalt precipitating peptides are under investigation. First results are promising and have demonstrated the feasibility to genetically engineer S-layer fusion proteins incorporating metal-binding peptides capable of forming monolayers on technologically important substrates such as silicon, glass, gold, or polymeric surfaces.

On the basis of the work on binding biomolecules, such as enzymes or antibodies, in S-layer-based biosensors, it has already been demonstrated that metallic and semiconducting nanoparticles can be bound in regular arrangements. The pattern of bound molecules and nanoparticles frequently reflects the lattice symmetry, the size of the morphological units, and the physicochemical properties of the array. Specific binding of molecules and nanoparticles on S-layer lattices may be induced by different noncovalent forces or, most recently, by genetically introduced, specific functional domains. For example, the distribution of net negatively charged domains on S-layers could be visualized by electron microscopical methods after labeling with positively charged topographical markers, such as polycationic ferritin (PCF; diameter, 12 nm) (3, 53). The regular arrangement of free carboxylic acid groups on the hexagonal S-layer lattice from *T. tenax* was clearly demonstrated in this way. Recently, gold- and amino-functionalized CdSe had been bound onto S-layer protein monolayers and self-assembly products of SbpA, the S-layer protein of *Ly. sphaericus* CCM 2177 (236). SbpA monolayers recrystallized on hydrophobic silicon surfaces expose the outer S-layer face toward the environment. Amino-functionalized 4-nm-sized CdSe particles were bound to EDC-activated carboxyl groups at

the outer S-layer face in register with the underlying square S-layer lattice (236). On hydrophilic silicon surfaces, SbpA forms double layers where the inner S-layer surfaces are facing each other and thus, again, expose their outer S-layer face toward the environment. The inner face is accessible only where the double layers are incomplete. Citrate-stabilized negatively charged gold nanoparticles of 5 nm in diameter were bound by electrostatic interactions at the inner S-layer face forming extended superlattices. In another example, the hexagonally packed intermediate (HPI) S-layer of *Deinococcus radiodurans* was used for the self-assembly of preformed gold nanoparticles into superlattices commensurate with the underlying S-layer lattice (237). Each hexamer is in the form of a hollow, cone-shaped protrusion with a positively charged central channel. High resolution transmission electron microscopy (TEM) studies showed that negatively charged monodisperse gold nanoparticles with mean sizes of ~ 8 and ~ 5 nm, respectively, were electrostatically bound at these sites forming crystalline domains. A major breakthrough in the controlled binding of molecules and nanoparticles was achieved by the successful design and expression of S-layer-streptavidin fusion proteins, which allowed a specific binding of biotinylated ferritin molecules into regular arrays (129). The fusion proteins had the inherent ability to self-assemble into monomolecular protein lattices. The fusion proteins and STV were produced independently in *E. coli*, and were isolated, purified, and mixed to refold into heterotetramers of 1:3 stoichiometry. Self-assembled chimeric S-layers could be formed in suspension, on liposomes, on silicon wafers, and on SCWP-containing cell wall fragments. The two-dimensional protein crystals displayed STV in defined repetitive spacing (Fig. 6b and c) and were capable of binding D-biotin and biotinylated proteins, in particular ferritin. Furthermore, it could be demonstrated that all fused STV functionalities had the same position and orientation within the unit cell and were exposed. Such chimeric S-layer protein lattices can be used as self-assembling nanopatterned molecular affinity matrices capable of arranging biotinylated compounds in ordered arrays on surfaces.

S-Layer neoglycoproteins. Glycosylation is the most frequent, and possibly, also the most important modification of native proteins in all domains of life. Protein glycosylation is, in many cases, the key to protein function in a biological context, regulating and influencing many cellular processes, such as recognition, signaling, trafficking, biological half-life, and adhesion events. Also, in the field of immunology, vital functions are enabled and enhanced through glycan signals on proteins (238, 239). Thus, engineering of tailor-made, bioactive glycoproteins (referred to as *neoglycoproteins*) will decisively change our capabilities in influencing and controlling complex biological systems. For enabling an interaction of physiologically relevant strength, the mode of glycan display with regard to spatial accessibility and glycan density are of great importance. On the basis of the finding that several S-layer proteins are naturally modified with glycan chains (compare with Section titled Biochemistry, Genetics, and

Structure), with the carbohydrates always facing the environment, we have chosen an approach in which we utilize the S-layer protein self-assembly portion of these glycoproteins as a unique matrix for the controllable, mono- or multivalent display of functional, bioactive glycans in high density with nanometer-scale periodicity (70). Following current trends in the conceptualization of novel self-assembly nanomaterials, it is evident that functional S-layer protein glycosylation is adding a new and very valuable component to an S-layer-based molecular construction kit.

In our long-term research strategy, the detailed knowledge of the S-layer protein matrix and of heterologous, functional glycosylation features, such as O-antigens or receptor mimics, shall converge. In principle, alteration of the native S-layer glycan or assembly of completely new glycans on permissive sites of the S-layer protein portion can be envisaged. In any case, the detailed and molecular understanding of the native S-layer protein glycosylation process is a prerequisite. Owing to the complexity of S-layer glycan biosynthesis, involving a large number of enzymes for nucleotide sugar biosynthesis, glycosyl transfer reactions, polymerization, membrane transfer of the oligosaccharide chain, and its ligation to distinct sites on the target protein, S-layer glycoproteins have escaped (nano)biotechnological applications so far.

To utilize an S-layer protein as a target for engineered glycosylation, on the basis of the knowledge of the amino acid sequence, the native glycosylation sites and potentially additional permissive sites for glycosylation have to be determined that allow introduction of exogenous glycosylation sequences into the S-layer protein that will be recognized by the respective protein:oligosaccharyltransferase. In addition, incorporation of structural or functional domains into the S-layer protein by protein engineering techniques allows tuning S-layer neoglycoprotein properties for specific purposes. Currently, several microorganisms from the *Bacillaceae* family are being investigated in detail for this endeavor.

Our strategy follows two principal lines of development. The first one is the *in vivo* display of functional glycans on the surface of bacteria enabled by means of recombinant DNA technology. This has become an increasingly used strategy in various applications in microbiology, nanobiotechnology, and vaccinology (240). Besides outer membrane proteins, lipoproteins, autotransporters, or subunits of surface appendages that are being evaluated for this kind of applications, the use of the S-layer (glyco)protein cell surface anchor is a very attractive and promising alternative. An impressive example related to this line of development was stated by Paton and coworkers (241), who demonstrated that a recombinant *E. coli* that displayed a Shiga toxin receptor mimic on its cell surface was capable of adsorbing and neutralizing Shiga toxins with very high efficiency. The *in vitro* line of development utilizes the recrystallization capability of the S-layer portion on a broad spectrum of supports. In either line, the S-layer “anchor” offers the unique advantage of providing a crystalline, regular matrix for the display of functional glycosylation motifs.

Currently, *G. stearothermophilus* NRS 2004/3a is the best investigated model organism for addressing questions

relevant for S-layer neoglycoprotein design. We have identified the initiation enzyme WsaP (85) and the oligosaccharyl:protein transferase WsaB, which catalyze the transfer of the elongated glycan chain to the S-layer protein acceptor sequence as key modules for S-layer neoglycoprotein design. Proof of concept of the recombinant production of S-layer neoglycoproteins was obtained after engineering the native O-glycosylation site of SgsE at amino acid residue threonine 620 into a target for N-glycosylation by introducing the 12-amino acid-long N-glycosylation sequence of the AcrA protein of *Campylobacter jejuni* (242), followed by the co-/posttranslational transfer of either the native AcrA heptasaccharide from *C. jejuni* or the O7 polysaccharide from *E. coli* by the action of the oligosaccharyl:protein transferase PglB from *C. jejuni* (243). In the chosen approach, the degree of glycosylation of the S-layer neoglycoproteins after purification from the periplasmic fraction of the expression host reached completeness and, most importantly for the envisaged applications, the S-layer neoglycoproteins fully maintained their self-assembling property according to the electron microscopic evidence. Tailor-made (“functional”) nanopatterned, self-assembling S-layer neoglycoproteins may open up new strategies for influencing and controlling complex biological systems based on carbohydrate recognition, with potential applications in the areas of biomimetics, drug targeting and delivery, vaccine design, or diagnostics. As S-layer neoglycoprotein production represents a fresh area of research, the benefits of S-layer neoglycoproteins for potential nanobiotechnology applications will have to be determined in the future.

S-Layers for Vaccine Development

Among different biotechnological and medical application aspects of S-layers, their use in vaccine formulation is obvious, because of the cell surface location. Since surface components frequently mediate specific interactions of a pathogen with its host organism, S-layers of pathogenic strains, in particular, are expected to have an important role in virulence (4). The experimental use of bacterial S-layers as attenuated pathogens, antigen/hapten carrier, adjuvants, or as part of vaccination vesicles has progressed in three areas of application: (i) antibacterial vaccines, (ii) immunotherapy of cancers, and (iii) antiallergic immunotherapy (for reviews see Refs (4, 244)).

In the case of fish vaccines, to fight *Aeromonas* infections, which can cause furunculosis in fish in freshwater and marine environments, the crystalline cell surface protein itself is considered as a good vaccine candidate. The S-layers of *A. salmonicida* and *A. hydrophila* are required for virulence, since isogenic mutants are avirulent (245). Numerous attempts have been undertaken to vaccinate salmon, trout, and catfish against furunculosis using whole cells, cell sonicates, and crude or partially purified cellular preparations (246–249). In this context, Ford and coworkers (249) showed that catfish were protected against experimental challenges with the homologous, virulent bacteria when immunization was performed with an S-layer-containing acid extract of *Aeromonas hydrophila* emulsified in Freund's incomplete adjuvants

(FIA). Infectious hematopoietic necrosis virus (IHNV) produces a severe hemorrhagic disease in young salmonid fish and is another severe threat for fish farming. A subunit model vaccine was developed by fusing a 184-amino acid segment of IHNV glycoprotein to the C-terminal portion of the S-layer protein of *Caulobacter crescentus* (250).

Another application of S-layers is their use as carrier for immunogenic antigens and haptens (46, 251). Since common carriers for peptide epitopes are used as monomers in solution (e.g. tetanus or diphtheria toxoids) or as dispersions of unstructured aggregates on aluminum salts, a reproducible immobilization of ligands to the carrier protein cannot be achieved (252, 253). Consequently, the use of regularly structured S-layer self-assembly products as immobilization matrices represents a completely new approach. Investigations focused on the development of several model conjugate vaccines with S-layer (glyco)proteins of thermophilic bacilli and clostridia and weekly immunogenic carbohydrate antigens, for example, *Streptococcus pneumoniae* serotype 8 poly- and oligosaccharides, haptens, or recombinant birch pollen allergen showed promising results in vaccination trials (38, 244, 254–257).

Immunization experiments in mice have indicated that S-layers served not only as carriers but also as adjuvants (257, 258). Allergen–S-layer conjugates and fusion proteins have been prepared with the intention to suppress the T-helper cell (Th2)-directed, IgE-mediated allergic responses to Bet v1, the major allergen of birch pollen (259). These studies showed that the S-layer protein conjugate induced interferon- γ (IFN- γ) production and, thus, activated the phagocytotic cells, which confirmed that Th1-enhancing properties are clearly attributable to the S-layer protein. Furthermore, the recombinant S-layer/Bet v1 fusion protein altered an established Th2-dominated phenotype as well as the *de novo* cytokine secretion profile toward a more balanced Th1/Th0-like phenotype (260, 261). These data clearly confirmed the immunomodulating properties of the S-layer moiety in S-layer fusion proteins and support the concept that recombinant fusion of allergens to S-layer proteins is a promising approach to improve vaccines for specific immunotherapy of atopic allergen.

Furthermore, there is an urgent need for new vaccines, allowing mucosal administration instead of intramuscular injections for the achievement of desired effects, such as adjuvant targeting, site-specific delivery, and controlled immune responses. S-layer-hapten conjugates induced significant vaccination responses even after oral/nasal administration. One project was directed to immunotherapy of cancer since conjugates of S-layer with small, tumor-associated oligosaccharides were found to elicit hapten specific delayed-type hypersensitivity (DTH) responses (256).

A further approach was the usage of recombinant S-layer fusion proteins and empty bacterial cell envelopes (ghosts) to deliver candidate antigens (Omp26) for a vaccine against nontypeable *Haemophilus influenzae* (NTHi) infection. The bacterial ghost system inducing Omp26-specific antibody response in mice is a novel vaccine delivery system endowed with intrinsic adjuvant properties (262).

S-layer self-assembly products and S-liposomes (209, 263) can be considered as particulate adjuvants with dimensions comparable to those of bacteria or viruses that the immune system evolved to combat. The mechanical and thermal stability of S-liposomes (263–265) and the possibility for immobilization or entrapping biologically active molecules (209, 266, 267) introduced a broad application potential, particularly as carrier and/or drug-delivery and drug targeting systems or in gene therapy, for example, as artificial viruses (4).

A number of vaccine approaches involve the development of vaccination vehicles, serving to potentiate the immune response to an antigen. To display foreign peptides on the *C. crescentus* cell surface in a dense, highly ordered structure, the hexagonal S-layer formed by the single secreted protein RsaA was exploited (268, 269). The *C. crescentus* RsaA secretion apparatus was used to produce a fusion protein composed of RsaA and the receptor-binding motif (adhesintope) of the *Pseudomonas aeruginosa* pilin. This presentation system could have many potential applications, such as the development of whole-cell vaccines, tumor suppressors, cellular adsorbents, and peptide display libraries (270–272). Furthermore, the 11-amino acids long epitope c-myc from the human c-myc protooncogene was successfully expressed in every S-layer subunit of the *Lb. brevis* S-layer (SlpA) while maintaining the S-layer lattice structure (273). With the S-layer-based surface display system developed in this study, it is possible to present a large number of antigen epitope molecules on the surface of each *Lb. brevis* cell. Thus, surface displaying of vaccines as part of an S-layer would be a very efficient way to present antigens to the mucosa-associated lymphoreticular tissue (273). Furthermore, delivery of antigens to mucosal surfaces by lactic acid bacteria is considered to offer a safe alternative to live attenuated pathogens because of their food grade status.

Another study used the S-layer protein genes of an S-layer synthesizing organism as a cell surface display system for vaccination purposes. A recombinant *B. anthracis* strain was constructed by integrating a translational fusion harboring DNA fragments encoding the cell wall targeting domain of the S-layer protein EA1 and tetanus toxin fragment C (ToxC) into the chromosome. The humoral immune response was sufficient to protect mice against tetanus toxin challenge (274).

Current studies focus on the production of S-layer fusion proteins between the S-layer proteins of *Ly. sphaericus* CCM 2177 and *G. stearothermophilus* PV72/p2 and peptide mimotopes such as F1 that mimics an immunodominant epitope of Epstein–Barr virus (EBV) (137). Screening of 83 individual sera that were EBV IgM-positive, EBV-negative, and potentially cross-reactive resulted in 98.2% specificity and 89.3% sensitivity as well as in no cross reactivity with related viral diseases. These results indicated the potential of these S-layer fusion proteins as a matrix for site-directed immobilization of small ligands in solid-phase immunoassays (137). A further approach concerns the construction of S-layer fusion proteins carrying the C-terminally fused antigen mpt64, a *Mycobacterium tuberculosis* protein, and their investigation to serve as adjuvant and carrier

for the vaccination against tuberculosis (H. Tschiggerl, unpublished data).

OUTLOOK AND PERSPECTIVES

The study and use of biological self-assembly systems is a rapidly growing scientific and engineering field that crosses the boundaries of biology, chemistry, physics, and material sciences. The innovation of such “bottom-up” processes lies in their capability to build uniform supramolecular structures with ultrasmall functional units and in the possibility to exploit such structures at the meso- and macroscopic scale (3, 7, 22).

It is now evident that from a theoretical point of view, S-layers are the simplest type of protein membrane. Since S-layer lattices possess repetitive physicochemical and morphological properties down to the subnanometer scale, they represent structures that exist at the ultimate resolution limit for the molecular functionalization of surfaces and interfaces.

So far, most biotechnological applications based on S-layers depend on the *in vitro* self-assembling capabilities of isolated S-layer subunits in suspension, on the surfaces of solids, lipid films, liposomes, and nanoparticles. Most importantly, S-layer recrystallization can be induced on flat surfaces and highly porous structures such as micro-filtration membranes or porous beads. Since the functional groups on S-layer lattices are aligned in well-defined positions and orientation, very precise chemical modifications and functionalization with molecules are possible (3).

Presently, the most important line of development concerns genetic manipulation of S-layer proteins and glycoproteins. Numerous studies have clearly demonstrated that S-layer proteins incorporating specific functional domains of proteins (e.g. enzymes, antibodies, antigens, ligands, and mimotopes) maintain the capability to assemble into coherent lattices on a great variety of solid supports. This strategy for “nanocontrolled” functionalization of surfaces leads to new enzyme and ultrafiltration membranes, affinity structures, ion-selective binding matrices, microcarriers, biosensors, diagnostics, biocompatible surfaces, mucosal vaccines, and encapsulation systems (9, 10).

An important area of future development concerned copying the supramolecular principle of cell envelopes of those archaea which possess S-layers as exclusive wall component. This biomimetic approach has led to a new technology for stabilizing functional lipid membranes and their use at meso- and macroscopic scale (5, 7, 8, 200). S-liposomes mimicking envelopes of human and animal viruses will lead to the development of new targeting, delivery, and encapsulation systems (8).

Although the progress in the development of S-layer technology primarily concerns life sciences, important areas emerge in non-life science applications. S-layer lattices allow the large-scale generation of arrays of metallic and semiconducting nanoparticle arrays as required for nanoelectronic or optical applications (275). Key is their use as matrices for the templated synthesis or binding of nanoparticles with specific optical, electronic,

catalytic, or structural properties. S-layer research provides novel materials and technologies for life and non-life science applications, which are superior to conventional approaches in terms of their fabrication efficiency.

Acknowledgments

This work was supported by the Austrian Science Fund (FWF, projects P16295-B10, P17170-B10, P18510-B12, P18013-B10, P19047-B12, P20256-B11, and P20605-B12) the EU, project NAS-SAP, the Austrian Federal Ministry of Transport, Innovation and Technology (MNA-Network), the Hochschuljubiläumsstiftung der Stadt Wien, project H-1809/2006, the Erwin Schrödinger Society for Nanosciences, and by the US Air Force Office of Scientific Research (AFOSR), projects F49620-03-1-0222, FA9550-06-1-0208, and FA9550-07-1-0313.

LIST OF ABBREVIATIONS

α HL	α -hemolysin
Bet v1	major birch pollen allergen
BLM	black lipid membrane
cAb	variable domain of a heavy chain camel antibody
CD	circular dichroism
DTH	delayed-type hypersensitivity
2-D	two-dimensional
3-D	three-dimensional
EBV	Epstein–Barr virus
EDC	1-ethyl-3,3'-(dimethylaminopropyl) carbodiimide
EGFP	enhanced green fluorescent protein
ELISA	enzyme-linked immunosorbent assay
F1	peptide mimotope of EBV epitope FIA Freund's incomplete adjuvants
HPI	hexagonally packed intermediate S-layer of <i>Deinococcus radiodurans</i>
HUVEC	human umbilical vein endothelial cells
IFN- γ	interferon- γ
Ig	immunoglobulin
IHNV	infectious hematopoietic necrosis virus
IL 8	interleukin 8
LamA	β -1,3-endoglucanase of <i>Pyrococcus furiosus</i>
LB	Langmuir–Blodgett
MS	mass spectrometry

NMR	nuclear magnetic resonance
NTHi	nontypeable <i>Haemophilus influenzae</i>
PCF	polycationic ferritin
PSA	prostate-specific antigen
QCM-D	quartz crystal microbalance with dissipation monitoring
RmlA	glucose-1-phosphate thymidyltransferase of <i>G. stearothermophilus</i> NRS 2004/3a
SAW	surface acoustic wave
SbpA	S-layer protein of <i>Lysinibacillus sphaericus</i> CCM 2177
SbsB	S-layer protein of <i>Geobacillus stearothermophilus</i> PV72/p2
SbsC	S-layer protein of <i>Geobacillus stearothermophilus</i> ATCC 12980
SgsE	S-layer protein of <i>Geobacillus stearothermophilus</i> NRS 2004/3a
SCWP	secondary cell wall polymer
SDS-PAGE	sodium dodecyl sulfate polyacrylamide gel electrophoresis
SLH	S-layer homology
S-liposome	S-layer-coated liposome
SPR	surface plasmon resonance
STI	strep-tag I
STV	streptavidin
SUM	S-layer ultrafiltration membrane
TEM	transmission electron microscopy
Th	T-helper cell
ToxC	tetanus toxin fragment C
t-PA	tissue type plasminogen activator
ZZ	Fc-binding domain of protein domain

REFERENCES

- Sleytr UB. *Int Rev Cytol* 1978; 53: 1–62.
- Sleytr UB, Messner P, Pum D, Sára M, editors. *Crystalline bacterial cell surface layers*. Berlin, Germany: Springer; 1988.
- Sleytr UB, Pum D, Schuster B, Sára M. In: Rosoff M, editor. *Nano-surface chemistry*. New York, Basle: Marcel Dekker; 2001. pp. 333–389.
- Sleytr UB, Sára M, Pum D, Schuster B, Messner P, Schäffer C. In: Steinbüchel A, Fahnstock S, editors. *Biopolymers*. Weinheim, Germany: Wiley-VCH; 2003. pp. 285–338.
- Schuster B, Sleytr UB. In: Tien TH, Ottova A, editors. *Advances in planar lipid bilayers and liposomes*. Amsterdam, The Netherlands: Elsevier Science; 2005. pp. 247–293.
- Sára M, Pum D, Huber C, Ilk N, Pleschberger M, Sleytr, U. In: Kumar C, editor. *Biological and pharmaceutical nanomaterials. Nanotechnologies for the life sciences*. Weinheim, Germany: Wiley-VCH; 2006. pp. 219–252.
- Sleytr UB, Egelseer EM, Ilk N, Pum D, Schuster B. *FEBS J* 2007; 274: 323–334.
- Sleytr UB, Huber C, Ilk N, Pum D, Schuster B, Egelseer EM. *FEMS Microbiol Lett* 2007; 267: 131–144.
- Egelseer EM, Sára M, Pum D, Schuster B, Sleytr UB. In: Shoseyov O, Levy I, editors. *NanoBioTechnology*. Totowa, NJ: Humana Press; 2008. pp. 55–86.
- Sleytr UB, Egelseer EM, Ilk N, Messner P, Schäffer C, Pum D, Schuster B. In: König H, Claus H, Varma A, editors. *Prokaryotic cell wall compounds - structure and biochemistry*. Heidelberg, Germany: Springer; in press.
- Sleytr UB, Beveridge TJ. *Trends Microbiol* 1999; 7: 253–260.
- Sleytr UB, Messner P, Pum D, Sára M. *Crystalline bacterial cell surface proteins*. Austin, TX: R. G. Landes Company and Academic Press; 1996.
- Murray, RGE. In: Beveridge TJ, Koval SF, editors. *Advances in bacterial paracrystalline surface layers*. New York, London: Plenum Press; 1993. pp. 3–9.
- Sleytr UB, Messner P, Pum D, Sára, M. In: Sleytr UB, Messner P, Pum D, Sára M, editors. *Crystalline bacterial cell surface proteins (S Layers)*. Austin, TX: R. G. Landes Company and Academic Press; 1996. pp. 5–33.
- Sleytr UB, Sára M, Pum D, Schuster B, Messner P, Schäffer C. In: Steinbüchel A, Fahnstock SR, editors. *Polyamides and complex proteinaceous materials I*. Weinheim, Germany: Wiley-VCH; 2002. pp. 285–338.
- Messner P, Egelseer EM, Schäffer C, Sleytr UB. In: König H, Claus H, Varma A, editors. *Prokaryotic cell wall compounds - structure and biochemistry*. Heidelberg, Germany: Springer; in press.
- Sleytr UB, Messner P. In: Schaechter M, editor. *Encyclopedia of microbiology*. San Diego, CA: Elsevier Science; in press.
- Baumeister W, Lembcke G, Dürr R, Phipps B. In: Fryer JR, Dorset DL, editors. *Electron crystallography of organic molecules*. Dordrecht, The Netherlands: Kluwer Academic Publishers; 1991. pp. 283–296.
- Hovmöller S. In: Beveridge TJ, Koval S, editors. *Advances in paracrystalline bacterial surface layers. Series A: life sciences*. New York: Plenum Press and NATO ASI Series; 1993. pp. 13–21.
- Beveridge TJ. *Curr Opin Struct Biol* 1994; 4: 204–212.
- Sleytr UB, Messner P. In: Plattner H, editor. *Electron microscopy of subcellular dynamics*. Boca Raton, FL: CRC Press; 1989. pp. 13–31.
- Sleytr UB, Sára M, Pum D, Schuster B. *Prog Surf Sci* 2001; 68: 231–278.
- Sleytr UB, Plohberger R. In: Baumeister W, Vogell W, editors. *Electron microscopy at molecular dimensions*. Berlin, Heidelberg, New York: Springer-Verlag; 1980. pp. 36–47.
- Sleytr UB. *FEMS Microbiol Rev* 1997; 20: 5–12.
- Sleytr UB, Messner P, Pum D, Sára M. *Angew Chem Int Ed* 1999; 38: 1034–1054.
- Sleytr UB, Sára, M, Pum D, Schuster B. In: Ciferri A, editors. *Supramolecular polymers*. Boca Raton, FL: 2005. pp. 583–612.
- Pum D, Sleytr UB. *Supramolec Sci* 1995; 2: 193–197.
- Györfvay ES, Stein O, Pum D, Sleytr UB. *J Microsc* 2003; 212: 300–306.
- Pum D, Weinhandl M, Hödl C, Sleytr UB. *J Bacteriol* 1993; 175: 2762–2766.

Q5

Q6

20 NANOTECHNOLOGICAL APPLICATIONS OF S-LAYERS

30. Schuster B, Sleytr UB. *Curr Nanosci* 2006; 2: 143–152.
31. Coelho MAN, Gliozzi A, Möhwald H, Perez E, Sleytr UB, Vogel H, Winterhalter M. *IEEE Trans Nanobiosci* 2004; 3: 3–5.
32. Sleytr UB, Györvary E, Pum D. *Prog Organ Coat* 2003; 47: 279–287.
33. Sleytr UB, Schuster B, Pum D. *IEEE Eng Med Biol* 2003; 22: 140–150.
34. Györvary E, O'Riordan A, Quinn A, Redmond G, Pum D, Sleytr UB. *Nano Lett* 2003; 3: 315–319.
35. Pum D, Wetzler B, Schuster B, Sleytr UB. In: Gourley PL, Kazir, A, editors. *Micro- and nanofabricated electro-optical mechanical systems for biomedical and environmental applications*. Bellingham, WA: SPIE; 1997. pp. 53–57.
36. Pum D, Sleytr UB. *Trends Biotechnol* 1999; 17: 8–12.
37. Sleytr UB, Messner P. *Annu Rev Microbiol* 1983; 37: 311–339.
38. Messner P, Sleytr UB. *Adv Microb Physiol* 1992; 33: 213–275.
39. Messner P. In: Sleytr UB, Messner P, Pum D, Sára M, editors. *Crystalline bacterial cell surface proteins*. Austin, TX: R. G. Landes Company and Academic Press; 1996. pp. 35–76.
40. Yamada H, Tsukagoshi N, Udaka S. *J Bacteriol* 1981; 148: 322–332.
41. Kist ML, Murray RG. *J Bacteriol* 1984; 157: 599–606.
42. Takeoka A, Takumi K, Koga T, Kawata T. *J Gen Microbiol* 1991; 137: 261–267.
43. Takumi K, Susami Y, Takeoka A, Oka T, Koga T. *Microbiol Immunol* 1991; 35: 569–575.
44. Hagiya H, Oka T, Tsuji H, Takumi K. *J Gen Appl Microbiol* 1992; 38: 63–74.
45. Peyret JL, Bayan N, Joliff G, Gulik-Krzywicki T, Mathieu L, Schechter E, Leblon G. *Mol Microbiol* 1993; 9: 97–109.
46. Sleytr UB, Messner P, Pum D, Sára M. *Mol Microbiol* 1993; 10: 911–916.
47. Messner P, Sleytr UB. In: Hancock IC, Poxton IR, editors. *Bacterial cell surface techniques*. Chichester: John Wiley & Sons; 1988. pp. 97–104.
48. Schuster B, Györvary E, Pum D, Sleytr UB. *Methods Mol Biol* 2005; 300: 101–123.
49. Koval SF, Murray RG. *Can J Biochem Cell Biol* 1984; 62: 1181–1189.
50. Sleytr UB. *Nature* 1975; 257: 400–402.
51. Beveridge TJ, Stewart M, Doyle RJ, Sprott GD. *J Bacteriol* 1985; 162: 728–737.
52. Sprott GD, Beveridge TJ, Patel GB, Ferrante G. *Can J Microbiol* 1986; 32: 847–854.
53. Messner P, Pum D, Sára M, Stetter KO, Sleytr UB. *J Bacteriol* 1986; 166: 1046–1054.
54. König H. In: Goodfellow M, O'Donnell AG, editors. *Chemical methods of prokaryotic systematics*. Chichester: John Wiley & Sons; 1994. pp. 85–119.
55. Kinns H, Howorka S. *J Mol Biol* 2008; 377: 589–604. DOI:10.1016/j.jmb.2008.01.019.
56. Dooley JS, McCubbin WD, Kay CM, Trust TJ. *J Bacteriol* 1988; 170: 2631–2638.
57. Dubreuil JD, Logan SM, Cabbage S, Eidhin DN, McCubbin WD, Kay CM, Beveridge TJ, Ferris FG, Trust TJ. *J Bacteriol* 1988; 170: 4165–4173.
58. Rünzler D, Huber C, Moll D, Köhler G, Sára M. *J Biol Chem* 2004; 279: 5207–5215.
59. Sára M. *Trends Microbiol* 2001; 9: 47–49.
60. Horejs C, Pum D, Sleytr UB, Tscheliessnig R. *J Chem Phys* 2008; 128: 065106. DOI:10.1063/1.2826375.
61. Sleytr UB, Sára M, Pum D. In: Ciferri A, editors. *Supramolecular polymers*. New York, Basel: Marcel Dekker; 2000. pp. 177–213.
62. Jarosch M, Egelseer EM, Huber C, Moll D, Mattanovich D, Sleytr UB, Sára M. *Microbiology* 2001; 147: 1353–1363.
63. Pavkov T, Oberer M, Egelseer EM, Sára M, Sleytr UB, Keller W. *Acta Crystallogr D Biol Crystallogr* 2003; 59: 1466–1468.
64. Pavkov T, Egelseer EM, Tesarz M, Svergun DI, Sleytr UB, Keller W. *Structure* in press.
65. Ferner-Ortner J, Mader C, Ilk N, Sleytr UB, Egelseer EM. *J Bacteriol* 2007; 189: 7154–7158.
66. Schäffer C, Messner P. *Microbiology* 2005; 151: 643–651.
67. Sumper M, Wieland FT. In: Montreuil J, Vliegenthart JFG, Schachter H, editors. *Glycoproteins*. Amsterdam, The Netherlands: Elsevier; 1995. pp. 455–473.
68. Schäffer C, Messner P. *Glycobiology* 2004; 14:31R–42R.
69. Eichler J, Adams MW. *Microbiol Mol Biol Rev* 2005; 69: 393–425.
70. Messner P, Steiner K, Zarschler K, Schäffer C. *Carbohydr Res* 2008; 343: 1934–1951. DOI:10.1016/j.carres.2007.12.025.
71. Thomas SR, Trust TJ. *J Mol Biol* 1995; 245: 568–581.
72. Mescher MF, Strominger JL. *J Biol Chem* 1976; 251: 2005–2014.
73. Sleytr UB, Thorne KJ. *J Bacteriol* 1976; 126: 377–383.
74. Raetz CR, Whitfield C. *Annu Rev Biochem* 2002; 71: 635–700.
75. Messner P, Schäffer C. In: Herz W, Falk H, Kirby GW, editors. *Progress in the chemistry of organic natural products*. Wien, Austria: Springer; 2003. pp. 51–124.
76. Sumper M, Berg E, Mengele R, Strobel I. *J Bacteriol* 1990; 172: 7111–7118.
77. Kärcher U, Schröder H, Haslinger E, Allmaier G, Schreiner R, Wieland F, Haselbeck A, König H. *J Biol Chem* 1993; 268: 26821–26826.
78. Voisin S, Houliston RS, Kelly J, Brisson JR, Watson D, Bardy SL, Jarrell KF, Logan SM. *J Biol Chem* 2005; 280: 16586–16593.
79. Abu-Qarn M, Yurist-Doutsch S, Giordano A, Trauner A, Morris HR, Hitchen P, Medalia O, Dell A, Eichler J. *J Mol Biol* 2007; 374: 1224–1236.
80. Schäffer C, Wugeditsch T, Kählig H, Scheberl A, Zayni S, Messner P. *J Biol Chem* 2002; 277: 6230–6239.
81. Novotny R, Pfösl A, Messner P, Schäffer C. *Glycoconj J* 2004; 20: 435–447.
82. Novotny R, Schäffer C, Strauss J, Messner P. *Microbiology* 2004; 150: 953–965.
83. Steiner K, Pohlentz G, Dreisewerd K, Berkenkamp S, Messner P, Peter-Katalinic J, Schäffer C. *J Bacteriol* 2006; 188: 7914–7921.
84. Bindila L, Steiner K, Schäffer C, Messner P, Mormann M, Peter-Katalinic J. *Anal Chem* 2007; 79: 3271–3279.
85. Steiner K, Novotny R, Patel K, Vinogradov E, Whitfield C, Valvano MA, Messner P, Schäffer C. *J Bacteriol* 2007; 189: 2590–2598.

86. Christian R, Schulz G, Unger FM, Messner P, Küpcü Z, Sleytr UB. *Carbohydr Res* 1986; 150: 265–272.
87. Sleytr UB, Messner P, Pum D, Sára M. In: Sleytr UB, Messner P, Pum D, Sára M, editos. *Crystalline bacterial cell surface proteins*. Austin, TX: R. G. Landes Company and Academic Press; 1996.
88. Radnedge L, Agron PG, Hill KK, Jackson PJ, Ticknor LO, Keim P, Andersen GL. *Appl Environ Microbiol* 2003; 69: 2755–2764.
89. Tu ZC, Zeitlin G, Gagner JP, Keo T, Hanna BA, Blaser MJ. *J Clin Microbiol* 2004; 42: 4405–4407.
90. Kato H, Yokoyama T, Arakawa Y. *J Med Microbiol* 2005; 54: 167–171.
91. Eidhin DN, Ryan AW, Doyle RM, Walsh JB, Kelleher D. *J Med Microbiol* 2006; 55: 69–83.
92. Poillane I, Humeniuk-Ainouz C, Durand I, Janoir C, Cruaud P, Delmee M, Popoff MR, Collignon A. *J Med Microbiol* 2007; 56: 386–390.
93. Sára M, Pum D, Küpcü S, Messner P, Sleytr UB. *J Bacteriol* 1994; 176: 848–860.
94. Boot HJ, Kolen CP, Pouwels PH. *J Bacteriol* 1995; 177: 7222–7230.
95. Boot HJ, Kolen CP, Pouwels PH. *Mol Microbiol* 1996; 21: 799–809.
96. Sára M, Kuen B, Mayer HF, Mandl F, Schuster KC, Sleytr UB. *J Bacteriol* 1996; 178: 2108–2117.
97. Dworkin J, Blaser MJ. *Mol Microbiol* 1997; 26: 433–440.
98. Cerquetti M, Molinari A, Sebastianelli A, Diociaiuti M, Petruzzelli R, Capo C, Mastrantonio P. *Microb Pathog* 2000; 28: 363–372.
99. Thompson SA, Blaser MJ. In: Nachamkin I, Blaser MJ, editors. *Campylobacter*. Washington, DC: ASM Press; 2000. pp. 321–347.
100. Calabi E, Ward S, Wren B, Paxton T, Panico M, Morris H, Dell A, Dougan G, Fairweather N. *Mol Microbiol* 2001; 40: 1187–1199.
101. Karjalainen T, Waligora-Dupriet AJ, Cerquetti M, Spigaglia P, Maggioni A, Mauri P, Mastrantonio P. *Infect Immun* 2001; 69: 3442–3446.
102. Mignot T, Mesnage S, Couture-Tosi E, Mock M, Fouet A. *Mol Microbiol* 2002; 43: 1615–1627.
103. Scholz HC, Riedmann E, Witte A, Lubitz W, Kuen B. *J Bacteriol* 2001; 183: 1672–1679.
104. Lupas A, Engelhardt H, Peters J, Santarius U, Volker S, Baumeister W. *J Bacteriol* 1994; 176: 1224–1233.
105. May A, Pusztahelyi T, Hoffmann N, Fischer RJ, Bahl H. *Arch Microbiol* 2006; 185: 263–269.
106. Ries W, Hotzy C, Schocher I, Sleytr UB, Sára M. *J Bacteriol* 1997; 179: 3892–3898.
107. Lemaire M, Miras I, Gounon P, Beguin P. *Microbiology* 1998; 144: 211–217.
108. Chauvaux S, Matuschek M, Beguin P. *J Bacteriol* 1999; 181: 2455–2458.
109. Ilk N, Kosma P, Puchberger M, Egelseer EM, Mayer HF, Sleytr UB, Sára M. *J Bacteriol* 1999; 181: 7643–7646.
110. Mesnage S, Tosi-Couture E, Mock M, Fouet A. *J Appl Microbiol* 1999; 87: 256–260.
111. Mesnage S, Fontaine T, Mignot T, Delepierre M, Mock M, Fouet A. *Embo J* 2000; 19: 4473–4484.
112. Egelseer EM, Danhorn T, Pleschberger M, Hotzy C, Sleytr UB, Sára M. *Arch Microbiol* 2001; 177: 70–80.
113. Cava F, de Pedro MA, Schwarz H, Henne A, Berenguer J. *Mol Microbiol* 2004; 52: 677–690.
114. Mader C, Huber C, Moll D, Sleytr UB, Sára M. *J Bacteriol* 2004; 186: 1758–1768.
115. Huber C, Ilk N, Rünzler D, Egelseer EM, Weigert S, Sleytr UB, Sára M. *Mol Microbiol* 2005; 55: 197–205.
116. Choudhury B, Leoff C, Saile E, Wilkins P, Quinn CP, Kannenberg EL, Carlson RW. *J Biol Chem* 2006; 281: 27932–27941.
117. Petersen BO, Sára M, Mader C, Mayer H, Sleytr UB, Pabst M, Puchberger M, Krause E, Hofinger A, Duus JO, Kosma P. *Carbohydr Res* (submitted).
118. Ilk N, Völlenklee C, Egelseer EM, Breitwieser A, Sleytr UB, Sára M. *Appl Environ Microbiol* 2002; 68: 3251–3260.
119. Egelseer EM, Leitner K, Jarosch M, Hotzy C, Zayni S, Sleytr UB, Sára M. *J Bacteriol* 1998; 180: 1488–1495.
120. Jarosch M, Egelseer EM, Mattanovich D, Sleytr UB, Sára M. *Microbiology* 2000; 146(Pt 2): 273–281.
121. Weis WI. *Curr Opin Struct Biol* 1997; 7: 624–630.
122. Avall-Jaaskelainen S, Palva A. *FEMS Microbiol Rev* 2005; 29: 511–529.
123. Smit E, Oling F, Demel R, Martinez B, Pouwels PH. *J Mol Biol* 2001; 305: 245–257.
124. Antikainen J, Anton L, Sillanpää J, Korhonen TK. *Mol Microbiol* 2002; 46: 381–394.
125. Ford MJ, Nomellini JF, Smit J. *J Bacteriol* 2007; 189: 2226–2237.
126. Sára M, Pum D, Schuster B, Sleytr UB. *J Nanosci Nanotechnol* 2005; 5: 1939–1953.
127. Pum D, Sleytr UB. *Colloids Surf A: Physicochem Eng Aspects* 1995; 102: 99–104.
128. Kuen B, Koch A, Asenbauer E, Sára M, Lubitz W. *J Bacteriol* 1997; 179: 1664–1670.
129. Moll D, Huber C, Schlegel B, Pum D, Sleytr UB, Sára M. *Proc Natl Acad Sci U S A* 2002; 99: 14646–14651.
130. Breitwieser A, Egelseer EM, Moll D, Ilk N, Hotzy C, Bohle B, Ebner C, Sleytr UB, Sára M. *Protein Eng* 2002; 15: 243–249.
131. Messner P, Pum D, Sleytr UB. *J Ultrastruct Mol Struct Res* 1986; 97: 73–88.
132. Schäffer C, Novotny R, Küpcü S, Zayni S, Scheberl A, Friedmann J, Sleytr UB, Messner P. *Small* 2007; 3: 1549–1559.
133. Huber C, Liu J, Egelseer EM, Moll D, Knoll W, Sleytr UB, Sára M. *Small* 2006; 2: 142–150.
134. Völlenklee C, Weigert S, Ilk N, Egelseer E, Weber V, Loth F, Falkenhagen D, Sleytr UB, Sára M. *Appl Environ Microbiol* 2004; 70: 1514–1521.
135. Ilk N, Küpcü S, Moncayo G, Klimt S, Ecker RC, Hofer-Warbinek R, Egelseer EM, Sleytr UB, Sára M. *Biochem J* 2004; 379: 441–448.
136. Tschiggerl H, Breitwieser A, de Roo G, Verwoerd T, Schäffer C, Sleytr UB. *J Biotechnol* 2008; 133: 403–411.
137. Tschiggerl H, Casey JL, Parisi K, Foley M, Sleytr UB. *Bioconjug Chem* 2008; 19: 860–865.
138. Huber C, Egelseer EM, Ilk N, Sleytr UB, Sára M. *Microelectron Eng* 2006; 83: 1589–1593.
139. Pleschberger M, Neubauer A, Egelseer EM, Weigert S, Lindner B, Sleytr UB, Muyltermans S, Sára M. *Bioconjug Chem* 2003; 14: 440–448.
140. Pleschberger M, Saerens D, Weigert S, Sleytr UB, Muyltermans S, Sára M, Egelseer EM. *Bioconjug Chem* 2004; 15: 664–671.

22 NANOBIOLOGICAL APPLICATIONS OF S-LAYERS

141. Blatt WF. In: Meares P, editor. Membrane separation process. Amsterdam, The Netherlands: Elsevier; 1976. pp. 81–120.
142. Mulder M, editor. Basic principles of membrane technology. Dordrecht, Boston: Kluwer Academic Publishers; 1991.
143. Sára M, Sleytr UB. *J Memb Sci* 1987; 33: 27–49.
144. Sára M, Sleytr UB. *J Bacteriol* 1987; 169: 4092–4098.
145. Manigley C, Wolf G, Sára M, Sleytr UB. In: Sleytr UB, Messner P, Pum D, Sára M, editors. Crystalline bacterial cell surface layers. Berlin, Germany: Springer-Verlag; 1988. pp. 154–159.
146. Sára M, Sleytr UB. In: Rehm HJ, editors. Biotechnology. Weinheim, Germany: Wiley-VCH; 1988. pp. 615–636.
147. Sleytr UB, Sára M. Structure with membrane having continuous pores. U.S. Patent 4,752,395. 1988.
148. Sleytr UB, Sára M. Use of structure with membrane having continuous pores. U.S. Pat. 4,849,109. 1989.
149. Sára M, Sleytr UB. *J Bacteriol* 1987; 169: 2804–2809.
150. Sára M, Pum D, Sleytr UB. *J Bacteriol* 1992; 174: 3487–3493.
151. Weigert S, Sára M. *J Memb Sci* 1995; 106: 147–159.
152. Küpcü S, Sára M, Sleytr UB. *J Memb Sci* 1991; 61: 167–175.
153. Sára M, Küpcü S, Weiner C, Weigert S, Sleytr UB. In: Sleytr UB, Messner P, Pum D, Sára M, editors. Immobilised macromolecules: application potentials. London, UK: Springer-Verlag; 1993. pp. 71–86.
154. Sára M, Küpcü S, Sleytr UB. In: Sleytr UB, Messner P, Pum D, Sára M, editors. Crystalline bacterial cell surface proteins. Austin, TX: R. G. Landes Company and Academic Press; 1996. pp. 133–159.
155. Weigert S, Sára M. *J Memb Sci* 1996; 121: 185–196.
156. Sára M, Sleytr UB. *Appl Microbiol Biotechnol* 1989; 30: 184–189.
157. Sára M, Küpcü S, Weiner C, Weigert S, Sleytr UB. In: Beveridge TJ, Koval SF, editors. Advances in bacterial paracrystalline surface layers. New York, London: Plenum Press; 1993.
158. Küpcü S, Mader C, Sára M. *Biotechnol Appl Biochem* 1995; 21: 275–286.
159. Crowther RA, Sleytr UB. *J Ultrastruct Res* 1977; 58: 41–49.
160. Sleytr UB, Sára M, Küpcü Z, Messner P. *Arch Microbiol* 1986; 146: 19–24.
161. Christian R, Messner P, Weiner C, Sleytr UB, Schulz G. *Carbohydr Res* 1988; 176: 160–163.
162. Bock K, Schuster-Kolbe J, Altman E, Allmaier G, Stahl B, Christian R, Sleytr UB, Messner P. *J Biol Chem* 1994; 269: 7137–7144.
163. Pum D, Sára M, Sleytr UB. In: Sleytr UB, Messner P, Pum D, Sára M, editors. Immobilised macromolecules: application potentials. London, UK: Springer-Verlag; 1993. pp. 141–160.
164. Neubauer A, Hödl C, Pum D, Sleytr UB. *Anal Lett* 1994; 27: 849–865.
165. Giraud MF, Naismith JH. *Curr Opin Struct Biol* 2000; 10: 687–696.
166. Koo OM, Rubinstein I, Onyukel H. *Nanomedicine* 2005; 1: 193–212.
167. Bora U, Sharma P, Kannan K, Nahar P. *J Biotechnol* 2006; 126: 220–229.
168. Hilal N, Kochkodan V, Nigmatullin R, Goncharuk V, Al-Khatib L. *J Memb Sci* 2006; 268: 198–207.
169. Breitwieser A, Küpcü S, Howorka S, Weigert S, Langer C, Hoffmann-Sommergruber K, Scheiner O, Sleytr UB, Sára M. *Biotechniques* 1996; 21: 918–925.
170. Weiner C, Sára M, Sleytr UB. *Biotechnol Bioeng* 1994; 43: 321–330.
171. Wilchek M, Bayer EA. Avidin-biotin technology. Orlando, FL: Academic Press; 1990.
172. Wilchek M, Bayer EA. In: Sleytr UB, Messner P, Pum D, Sára M, editors. Immobilised macromolecules: application potentials. London, UK: Springer-Verlag; 1993. p. 51.
173. Sleytr UB, Sára M. *Trends Biotechnol* 1997; 15: 20–26.
174. Breitwieser A, Mader C, Schocher I, Hoffmann-Sommergruber K, Aberer W, Scheiner O, Sleytr UB, Sára M. *Allergy* 1998; 53: 786–793.
175. Sleytr UB, Pum D, Sára M, Schuster B. In: Nalwa HS, editors. Encyclopedia of nanoscience and nanotechnology. San Diego, CA: Academic Press; 2004. pp. 693–702.
176. Völkel D, Zimmermann K, Breitwieser A, Pable S, Glatzel M, Scheifinger F, Schwarz HP, Sára M, Sleytr UB, Dorner F. *Transfusion* 2003; 43: 1677–1682.
177. Singer SJ, Nicolson GL. *Science* 1972; 175: 720–731.
178. Bowie JU. *Nature* 2005; 438: 581–589.
179. Engelman DM. *Nature* 2005; 438: 578–580.
180. McLaughlin S, Murray D. *Nature* 2005; 438: 605–611.
181. Papahadjopoulos D, Allen TM, Gabizon A, Mayhew E, Matthay K, Huang SK, Lee KD, Woodle MC, Lasic DD, Redemann C, *et al.* *Proc Natl Acad Sci U S A* 1991; 88: 11460–11464.
182. Puff N, Angelova MI. In: Tien TH, Ottova A, editors. Advances in planar lipid bilayers and liposomes. Amsterdam, The Netherlands: Elsevier Science; 2005. pp. 173–228.
183. Brezesinski G, Möhwald H. *Adv Colloid Interface Sci* 2003; 100–102: 563–584.
184. Cohen FS, Melikyan GB. *J Membr Biol* 2004; 199: 1–14.
185. Ottova A, Tien TH. In: Ottova A, Tien TH, editors. Advances in planar lipid bilayers and liposomes. Amsterdam, The Netherlands: Elsevier Science; 2005. pp. 221–245.
186. Sugawara M, Hirano A. In: Ottova A, Tien TH, editors. Advances in planar lipid bilayers and liposomes. Amsterdam, The Netherlands: Elsevier Science; 2005. pp. 221–245.
187. Sakmann B. *Pflugers Arch* 2006; 453: 249–259.
188. Morera FJ, Vargas G, Gonzalez C, Rosenmann E, Latorre R. *Methods Mol Biol* 2007; 400: 571–585.
189. Johansson E, Engvall C, Arfvidsson M, Lundahl P, Edwards K. *Biophys Chem* 2005; 113: 183–192.
190. Carmona-Ribeiro AM. *Curr Med Chem* 2006; 13: 1359–1370.
191. Sackmann E. *Science* 1996; 271: 43–48.
192. Sackmann E, Tanaka M. *Trends Biotechnol* 2000; 18: 58–64.
193. Schuster B, Sleytr UB. *Rev Mol Biotechnol* 2000; 74: 233–254.
194. Sinner EK, Knoll W. *Curr Opin Chem Biol* 2001; 5: 705–711.
195. Richter RP, Him JL, Brisson AR. *Mater Today* 2003; 6: 32–37.
196. Schuster B, Gufler PC, Pum D, Sleytr UB. *IEEE Trans Nanobiosci* 2004; 3: 16–21.
197. Schuster B. *NanoBiotechnology* 2005; 1: 153–164.
198. Tanaka M, Sackmann E. *Nature* 2005; 437: 656–663.
199. Chan YH, Boxer SG. *Curr Opin Chem Biol* 2007; 11: 581–587.

200. Schuster B, Sleytr UB. In: Bernstein EM, editors. Bioelectrochemistry research developments. Hauppauge: Nova Science Publishers; 2008. pp. 105–124.
201. Bakker-Woudenberg IA. *Int J Antimicrob Agents* 2002; 19: 299–311.
202. Ge L, Möhwald H, Li J. *Colloids Surf A: Physicochem Eng Aspects* 2003; 221: 49–53.
203. Zhang L, Granick S. *Nano Lett* 2006; 6: 694–698.
204. Celli A, Lee CY, Gratton E. *Methods Mol Biol* 2007; 400: 333–339.
205. Zhang L, Dammann K, Bae SC, Granick S. *Soft Matter* 2007; 3: 551–553.
206. Kashefi K, Lovley DR. *Science* 2003; 301: 934.
207. Stetter KO. *Extremophiles* 2006; 10: 357–362.
208. Sleytr UB, Egelseer EM, Pum D, Schuster B. In: Niemeyer CM, Mirkin CA, editors. *NanoBiotechnology: concepts, methods and perspectives*. Weinheim, Germany: Wiley-VCH; 2004. pp. 77–92.
209. Küpcü S, Sára M, Sleytr UB. *Biochim Biophys Acta* 1995; 1235: 263–269.
210. Schuster B, Pum D, Sára M, Braha O, Bayley H, Sleytr UB. *Langmuir* 2001; 17: 499–503.
211. Hirn R, Schuster B, Sleytr UB, Bayerl TM. *Biophys J* 1999; 77: 2066–2074.
212. Wetzler B, Pfandler A, Györvary E, Pum D, Lösche M, Sleytr UB. *Langmuir* 1998; 14: 6899–6906.
213. Pum D, Sleytr UB. *Thin Solid Films* 1994; 244: 882–886.
214. Schuster B, Pum D, Sára M, Sleytr UB. *Mini Rev Med Chem* 2006; 6: 909–920.
215. Györvary E, Wetzler B, Sleytr UB, Sinner A, Offenhäusser A, Knoll W. *Langmuir* 1999; 15: 1337–1347.
216. Janshoff A, Steinem C. *Anal Bioanal Chem* 2006; 385: 433–451.
217. Viviani B, Gardoni F, Marinovich M. *Int Rev Neurobiol* 2007; 82: 247–263.
218. Ellis C, Smith A. *Nat Rev Drug Discov* 2004; 3: 238–278.
219. Schuster B, Pum D, Sleytr UB. *Biochim Biophys Acta* 1998; 1369: 51–60.
220. Schuster B, Weigert S, Pum D, Sára M, Sleytr UB. *Langmuir* 2003; 19: 2392–2397.
221. Gufler PC, Pum D, Sleytr UB, Schuster B. *Biochim Biophys Acta* 2004; 1661: 154–165.
222. Bhakdi S, Tranum-Jensen J. *Microbiol Rev* 1991; 55: 733–751.
223. Schuster B, Pum D, Braha O, Bayley H, Sleytr UB. *Biochim Biophys Acta* 1998; 1370: 280–288.
224. Schuster B, Sleytr UB. *Bioelectrochemistry* 2002; 55: 5–7.
225. Douglas K, Clark NA, Rothschild KJ. *Appl Phys Lett* 1986; 48: 676–678.
226. Douglas S, Beveridge TJ. *FEMS Microbiol Ecol* 1998; 26: 79–88.
227. Shenton W, Pum D, Sleytr UB, Mann S. *Nature* 1997; 389: 585–587.
228. Dieluweit S, Pum D, Sleytr UB. *Supramolec Sci* 1998; 5: 15–19.
229. Mertig M, Kirsch R, Pompe W, Engelhardt H. *Eur Phys J D* 1999; 9: 45–48.
230. Mertig M, Wahl R, Lehmann M, Simon P, Pompe W. *Eur Phys J D* 2001; 16: 317–320.
231. Wahl R, Mertig M, Raff J, Selenska-Pobell S, Pompe W. *Adv Mat Sci Technol* 2001; 13: 736–740.
232. Bergkvist M, Mark SS, Yang X, Angert ER, Batt CA. *J Phys Chem B* 2004; 108: 8241–8248.
233. Dieluweit S, Pum D, Sleytr UB, Kautek W. *Mat Sci Eng C* 2005; 25: 727–732.
234. Naik RR, Stringer SJ, Agarwal G, Jones SE, Stone MO. *Nat Mater* 2002; 1: 169–172.
235. Naik RR, Jones SE, Murray CJ, McAuliffe JC, Vaia RA, Stone MO. *Adv Funct Mater* 2004; 14: 25–30.
236. Györvary E, Schroedter A, Talapin DV, Weller H, Pum D, Sleytr UB. *J Nanosci Nanotechnol* 2004; 4: 115–120.
237. Hall SR, Shenton W, Engelhardt H, Mann S. *ChemPhys Chem* 2001; 3: 184–186.
238. Apweiler R, Hermjakob H, Sharon N. *Biochim Biophys Acta* 1999; 1473: 4–8.
239. Spiro RG. *Glycobiology* 2002; 12: 43R–56R.
240. Samuelson P, Gunneriusson E, Nygren PA, Stahl S. *J Biotechnol* 2002; 96: 129–154.
241. Paton AW, Morona R, Paton JC. *Nat Med* 2000; 6: 265–270.
242. Feldman MF, Wacker M, Hernandez M, Hitchen PG, Marolda CL, Kowarik M, Morris HR, Dell A, Valvano MA, Aebi M. *Proc Natl Acad Sci U S A* 2005; 102: 3016–3021.
243. Steiner K, Hanreich A, Kainz B, Hitchen PG, Dell A, Messner P, Schäffer C. *Small* (in press) doi:10.1002/smll.200701215.
244. Messner P, Unger FM, Sleytr UB. In: Sleytr UB, Messner P, Pum D, Sára M, editors. *Crystalline bacterial cell surface proteins*. Austin, TX: R.G. Landes. Academic Press; 1996. pp. 161–173.
245. Kay WW, Trust TJ. *Experientia* 1991; 47: 412–414.
246. Udey LR, Fryer JL. *Mar Fish Rev* 1978; 40: 12–17.
247. Evenberg D, De Graaff P, Lugtenberg B, Van Muiswinkel WB. *J Fish Dis* 1988; 11: 337–350.
248. Thronton JC, Garduno RA, Newman SG, Kay WW. *Microb Pathog* 1991; 11: 85–99.
249. Ford LA, Thune RL. *Biomed Lett* 1992; 47: 355–362.
250. Simon B, Nomellini JF, Chiou P, Binale W, Thornton J, Smit J, Leong JA. *Dis Aquat Organ* 2001; 44: 400–402.
251. Sleytr UB, Mundt W, Messner P. US Patent Nr. 5,043,158 (1991).
252. Brown F, Hoey DGEM, Martin S, Rima BK, Trudgett A. *Vaccine design*. England, UK: John Wiley & Sons; 1993.
253. Powell MF, Newman MJ. *Vaccine design: the subunit and adjuvant approach*. New York: Plenum Press; 1995.
254. Malcolm AJ, Best MW, Szarka RJ, Mosleh Z, Unger FM, Messner P, Sleytr UB. In: Beveridge J, Koval SF, editors. *Bacterial paracrystalline surface layers*. New York: Plenum Press; 1993. pp. 219–233.
255. Malcolm AJ, Messner P, Sleytr UB, Smith RH, Unger FM. In: Sleytr UB, Messner P, Pum D, Sára M, editors. *Immobilized macromolecules: application potentials*. London, UK: Springer-Verlag; 1993. pp. 195–207.
256. Smith RH, Messner P, Lamontagne LR, Sleytr UB, Unger FM. *Vaccine* 1993; 11: 919–924.
257. Jahn-Schmid B, Siemann U, Zenker A, Bohle B, Messner P, Unger FM, Sleytr UB, Scheiner O, Kraft D, Ebner C. *Int Immunol* 1997; 9: 1867–1874.
258. Jahn-Schmid B, Messner P, Unger FM, Sleytr UB, Scheiner O, Kraft D. *J Biotechnol* 1996; 44: 225–231.
259. Jahn-Schmid B, Graninger M, Glözik M, Küpcü S, Ebner C, Unger FM, Sleytr UB, Messner P. *Immunotechnology* 1996; 2: 103–113.

24 NANOBIOLOGICAL APPLICATIONS OF S-LAYERS

260. Bohle B, Breitwieser A, Zwölfer B, Jahn-Schmid B, Sára M, Sleytr UB, Ebner C. *J Immunol* 2004; 172: 6642–6648.
261. Gerstmayr M, Ilk N, Schabussova I, Jahn-Schmid B, Egelseer EM, Sleytr UB, Ebner C, Bohle B. *J Immunol* 2007; 179: 7270–7275.
262. Riedmann EM, Kyd JM, Smith AM, Gomez-Gallego S, Jalava K, Cripps AW, Lubitz W. *FEMS Immunol Med Microbiol* 2003; 37: 185–192.
263. Mader C, Küpcü S, Sára M, Sleytr UB. *Biochim Biophys Acta* 1999; 1418: 106–116.
264. Küpcü S, Lohner K, Mader C, Sleytr UB. *Mol Membr Biol* 1998; 15: 69–74.
265. Hianik T, Küpcü S, Sleytr UB, Rybar P, Krivanek R, Kaatze U. *Coll Surf A* 1999; 147: 331–339.
266. Mader C, Kupcu S, Sleytr UB, Sára M. *Biochim Biophys Acta* 2000; 1463: 142–150.
267. Krivanek R, Rybar P, Küpcü S, Sleytr UB, Hianik T. *Bioelectrochemistry* 2002; 55: 57–59.
268. Bingle WH, Nomellini JF, Smit J. *Mol Microbiol* 1997; 26: 277–288.
269. Umelo-Njaka E, Nomellini JF, Bingle WH, Glasier LG, Irvin RT, Smit J. *Vaccine* 2001; 19: 1406–1415.
270. Georgiou G, Stathopoulos C, Daugherty PS, Nayak AR, Iverson BL, Curtiss R III. *Nat Biotechnol* 1997; 15: 29–34.
271. Nomellini JF, Toporowski MC, Smit J. In: Banex F, editors. *Expression technologies: current status and future trends*. Norfolk, UK: Horizon Scientific Press; 2004. pp. 477–524.
272. Bhatnagar PK, Awasthi A, Nomellini JF, Smit J, Suresh MR. *Cancer Biol Ther* 2006; 5: 485–491.
273. Avall-Jääskeläinen S, Kylä-Nikkilä K, Kahala M, Miikkulainen-Lahti T, Palva A. *Appl Environ Microbiol* 2002; 68: 5943–5951.
274. Mesnage S, Weber-Levy M, Haustant M, Mock M, Fouet A. *Infect Immun* 1999; 67: 4847–4850.
275. Pum D, Sleytr UB. In: Offenhäusser A, Rinaldi R, editors. *Nanobioelectronics for electronics, biology, and medicine*. Berlin, Germany: Springer; in press.

FURTHER READING

- Beveridge TJ, Koval SF, editors. *Advances in bacterial paracrystalline surface layers*. New York, London: Plenum Press; 1993.
- Egelseer EM, Sára M, Pum D, Schuster B, Sleytr UB. In: Shoseyov O, Levy I, editors. *Nanobiotechnology*. Totowa, NJ: Humana Press; 2008. pp. 55–86.
- Sára M, Egelseer EM, Huber C, Ilk N, Pleschberger M, Pum D, Sleytr UB. In: Bernd PN, editors. *Microbial bionanotechnology: biological self-assembly systems and biopolymer-based nanostructures, horizon bioscience*. New Zealand: Rehm Massey University; 2006. pp. 307–338.
- Schuster B, Sleytr UB. In: Tien T H, Ottova A., editors. *Advances in planar lipid bilayers and liposomes*. Amsterdam, The Netherlands: Elsevier Science; 2005. pp. 247–293.
- Sleytr UB, Egelseer EM, Ilk N, Pum D, Schuster B. *FEBS J* 2007; 274: 323–334.
- Sleytr UB, Huber C, Ilk N, Pum D, Schuster B, Egelseer EM. *FEMS Microbiol Lett* 2007; 267: 131–144.
- Sleytr UB, Messner P, Pum D, Sára M. *Immobilised macromolecules: application potentials*. London, UK: Springer-Verlag; 1993.
- Sleytr UB, Messner P, Pum D, Sára M. *Crystalline bacterial cell surface proteins*. Austin, TX: R. G. Landes Company and Academic Press; 1996.
- Sleytr UB, Messner P. In: Schaechter M, editors. *The desk encyclopedia of microbiology*. Amsterdam, The Netherlands: Elsevier; 2003. pp. 286–293.
- Sleytr UB, Pum D, Schuster B, Sára M. In: Rosoff M, editors. *Nano-surface chemistry*. New York, Basle: Marcel Dekker; 2001. pp. 333–389.
- Sleytr UB, Sára M, Pum D, Schuster B, Messner P, Schäffer C. In: Steinbüchel A, Fahnstock SR, editors. *Polyamides and complex proteinaceous materials I*. Weinheim, Germany: Wiley-VCH; 2002. pp. 285–338.
- Sleytr UB, Sára M, Pum D, Schuster B. In: Ciferri A, editors. *Supramolecular polymers*. Boca Raton, FL: 2005. pp. 583–612.

Queries in Chapter A

- Q1. Please provide abstract for this article.
- Q2. Please rephrase this part of the sentence "...glycosylation and phosphorylation have been found, with the former, rather complex modification being the most frequent one" for clarity.
- Q3. Please spell out this abbreviation (ORF) at the first instance.
- Q4. Please spell out this abbreviation (TRAE) at the first instance.
- Q5. Please clarify if this article has since been published. If so, please provide the year of publication for the references 10, 16, 17 and 275.
- Q6. Please provide the publisher's name for reference 26.
- Q7. Please clarify if this article has since been published. If so, please provide the volume number and page range for references 64, 117 and 243.